



Research paper

Parameter estimation of PV solar cells and modules using Whippy Harris Hawks Optimization Algorithm



Maryam Naeijian^a, Abolfazl Rahimnejad^b, S. Mohammadreza Ebrahimi^a, Nafiseh Pourmousa^c, S. Andrew Gadsden^{b,*}

^a Department of Electrical Engineering, Babol Noshirvani University of Technology, Babol, Iran

^b Department of Engineering Systems and Computing, University of Guelph, Guelph, Canada

^c Faculty of Electrical Engineering, Iran University of Science and Technology, Tehran, Iran

ARTICLE INFO

Article history:

Received 22 March 2021

Received in revised form 20 June 2021

Accepted 28 June 2021

Available online 8 July 2021

Keywords:

Solar cell
Single-diode model
Double-diode model
Three-diode model
Harris Hawks Optimization
RTC France photovoltaic cell
Photowatt-PWP 201 photovoltaic module
SM55
KC200GT
SW255

ABSTRACT

The significant global trend towards solar energy has led to the development of studies on the fabrication of high-performance solar cells. Accurate modeling and parameter identification of solar cells is of paramount importance. So far, several models have been proposed for the solar cell, including single-diode model (SDM), double-diode model (DDM), and three-diode model (TDM). Each model has a number of unknown parameters and several methods have been presented in the literature to find their optimal values. In this paper, an efficient optimization algorithm, namely Whippy Harris Hawks Optimization (WHHO), is proposed to estimate the model parameters of solar systems. The proposed WWHO is an enhanced version of the HHO algorithm and has the advantages of high convergence speed, global search capability, and high robustness over the original method. To evaluate the efficiency of the proposed WWHO algorithm, it is utilized to identify the parameters of various models of solar cells, and photovoltaic (PV) module. The results are compared with those obtained from a number of other recently presented optimization methods, which shows the superiority of the proposed algorithm. Furthermore, the effectiveness of WWHO algorithm in the practical application has been assessed for the parameter estimation of three commonly-used commercial modules under different irradiance and temperature conditions, which yield variations in the parameters of the PV model. The results obtained from various experimental setups confirm the high performance and robustness of the proposed algorithm.

© 2021 The Authors. Published by Elsevier Ltd. This is an open access article under the CC BY-NC-ND license (<http://creativecommons.org/licenses/by-nc-nd/4.0/>).

1. Introduction

Fossil fuels are one of the most widely used sources of energy because of their relatively high efficiency, ease of access, and transportation. However, various utilization of these fuels has led to some irreversible environmental damages, including air pollution, ozone depletion, emissions, climate change, and global warming (Imani et al., 2018a,b, 2019; Nasouri Gilvaei et al., 2021). Hence, the trend towards renewable energy sources (RESs) such as solar energy, wind energy, hydroelectric energy, and gravitational energy has significantly increased. RESs generate green energy with minimal damage to the environment. Solar energy is currently the third common source of energy throughout the world, which is widely used in various countries. The advantages of photovoltaic (PV) systems include easy installation, low maintenance costs, inexhaustible energy supply, noiseless generator,

and flexible sizes (Malekzadeh et al., 2020b). Furthermore, the production cost of solar cells (in dollars per watt) has decreased significantly, specifically during recent years. To be more precise numerically, in 1977, this production cost was \$76.67 per watt (\$/watt), and it dropped to 0.37 \$/watt, in 2017. These advantages have made PV energy systems the second green source of energy worldwide after wind energy systems. By the end of 2016, PV installation grew by 50%, reaching an installed capacity of 306.5 GW, and by the end of 2017, the PV installed capacity around the world has an increment of 80 GW. It is anticipated that during 2021, this amount will grow faster so that the installed capacity will reach 1 terawatt by the end of 2021 (Ebrahimi et al., 2019b; Ibrahim et al., 2020; Selem et al., 2021; Hasanien, 2015a; Qais et al., 2019b; Alam et al., 2015; Kumar et al., 2020; Chenouard and El-Sehiemy, 2020).

A PV cell is made of a junction of p-type and n-type semiconductors, and a PV module is made of a series and parallel connection of PV cells. The output power of a PV module depends on the number of PV cells used in its construction as well as environmental conditions such as temperature and irradiance

* Corresponding author.

E-mail address: gadsden@uoguelph.ca (S.A. Gadsden).

(Ebrahimi et al., 2019b). Due to the many advances that have been made in this field, PV applications have expanded from small scale, i.e., a small number of PV cells, to large scale, i.e., a large number of PV modules (Chenouard and El-Sehiemy, 2020). Due to the growing trend towards PV systems, they need to be studied and analyzed comprehensively from various points of view. Many researchers have carried out different studies to identify and resolve the issues with PV systems so as to reduce the overall costs while maintaining (or even increasing) their efficiency (Rizk-Allah and El-Fergany, 2020).

One of the most important and challenging issues with PV systems is the accurate and efficient modeling of solar cells (and PV modules). These issues are mainly caused by the nonlinear characteristics of solar cells, as well as the unavailability of all their parameters (Yousri et al., 2020; Chenche et al., 2018). In order to properly analyze and evaluate the actual behavior of PV systems, we need to derive an accurate model to be used in the simulation studies. The extracted model can be utilized to design a high-performance controller and optimize the PV system operation (Lin and Wu, 2020). Several mathematical models have been proposed to describe the PV characteristics under different operating conditions, the most common of which is the diode-based model. The single-diode model (SDM) is the simplest model with 5 unknown parameters (Chegaar et al., 2001; Villalva et al., 2009; Cárdenas et al., 2016). The double-diode model (DDM) considers more details than the SDM and has 7 unknown parameters (Chan and Phang, 1987; Mathew et al., 2017; Ishaque et al., 2011b). The three-diode model (TDM) is even a more accurate model since it considers the effects of the leakage current coefficients, grain boundaries, and carrier recombination (Ibrahim et al., 2020); the TDM has 9 unknown parameters (Abd Elaziz and Oliva, 2018; Allam et al., 2016; Khanna et al., 2015). In recent years, another model, namely multi-diode model, has been proposed to better model different PV technologies; this model consists of m parallel diodes and the number of its unknown parameters is $2m+3$ (Lim et al., 2015; Nishioka et al., 2007; Nunes et al., 2018). Furthermore, a multi-dimension diode PV model is presented in Soon and Low (2015); this model is an organized network consisting of a large number of series and parallel diodes and has high accuracy. Obviously, as the number of unknown parameters of the model increases, its accuracy and complexity increase. The appropriate model is selected according to the type of PV application and also a compromise between model accuracy and model simplicity (Ibrahim et al., 2020). The more accurate we estimate the unknown parameters of the PV model, the better the performance and control of the PV system (closer to optimal operating point) will be (Chenouard and El-Sehiemy, 2020).

Several methods have been proposed in the literature to estimate the parameters of PV cell/module. These methods are generally divided into two categories: deterministic and heuristic methods. Deterministic methods themselves are classified into analytical and iterative methods (Waly et al., 2019). Analytical methods utilize PV datasheet information (maximum voltage V_m , maximum current I_m , maximum power P_m , short circuit current I_{sc} , open-circuit voltage V_{oc}) or its I-V characteristic curve to formulate the parameter estimation problem (Chenouard and El-Sehiemy, 2020; Chan et al., 1986; Saleem and Karmalkar, 2009; Ortiz-Conde et al., 2006). Some examples of analytical methods include Reduced Space Search (RSS) (Cárdenas et al., 2016), Lambert-W-based methods (Chenche et al., 2018), and OSMP based methods (Tong and Pora, 2016). These methods are complex and time-consuming because they determine the unknown parameters of the PV cell model by solving nonlinear equations; the computational complexity of the analytical method will dramatically increase by increasing the number of unknown parameters of the PV model. In order to reduce the complexity

of nonlinear equations, a set of simplifications may be applied to the model. For instance, a constant value may be considered for R_s and R_{sh} (Celik and Acikgoz, 2007) or they may be neglected in the problem formulation (Di Piazza et al., 2017; Hejri et al., 2014; Babu and Gurjar, 2014); this can lead to an inaccurate estimation result. Another category of deterministic methods is the iterative methods in which parameters are obtained by trial and error or iteration (Salahshour et al., 2019a,b). These methods include Newton-Raphson method (Ayang et al., 2019; Yahya-Khotbehsara and Shahhoseini, 2018; Easwarakhanthan et al., 1986), Gauss-Seidel method (Chatterjee et al., 2011), and least squares method (El Achoubi et al., 2018; Toledo et al., 2018). To use the iterative methods, the equations of the system have to be convex, continuous, and differentiable; this restricts the application of these methods. Moreover, selecting the appropriate initial values in iterative methods is of paramount importance so that a wrong choice may lead to getting stuck in local optima (Kler et al., 2019; Qais et al., 2020; Malekzadeh et al., 2016).

Due to the above-mentioned weaknesses of deterministic methods, researchers turned to heuristic methods, in which the unknown parameters of the PV model are obtained by solving an optimization problem. In fact, by defining a suitable objective function, unknown parameters are obtained in such a way that the objective function is minimized (Jordehi, 2016). In heuristic methods, the problem of parameter estimation is treated as a black-box type problem, in which there is no need to apply some simplifications (or restrictions) to the system equations, unlike deterministic methods. According to the literature, various heuristic methods have been successfully applied to extract PV parameters, some of which are listed as follows: Genetic Algorithm (GA) (Ismail et al., 2013), Simulated Annealing (SA) (El-Naggar et al., 2012), Artificial Bee Colony Algorithm (ABC) (Oliva et al., 2014), Artificial Bee Swarm Optimization (ABSO) (Askarzadeh and Rezazadeh, 2013a; Gholipour et al., 2015), Harmony Search-based Algorithm (HS) (Askarzadeh and Rezazadeh, 2012), Particle Swarm Optimization (PSO) (Ye et al., 2009; Nunes et al., 2018; Gholipour et al., 2012a,b), Sunflower Optimization (SFO) (Qais et al., 2019a), Moth-Flame Optimizer (MFO) (Allam et al., 2016), Salp Swarming Algorithm (SSA) (Abbassi et al., 2019), Whale Optimizer (Elazab et al., 2018), Flower-Pollinating Optimization (FPO) (Alam et al., 2015), Jaya optimization (Yu et al., 2019), water cycling optimization (Kler et al., 2017), Wind Driven Optimization (WDO) (Derick et al., 2017), Innovative Global Harmony Search (IGHS) (Askarzadeh and Rezazadeh, 2012), Bird Mating Optimizer (BMO) (Askarzadeh and Rezazadeh, 2013b), Mine Blast Algorithm (MBA) (El-Fergany, 2015), Cat Swarm Optimization (CSO) (Guo et al., 2016), Teaching Learning Based Optimization (TLBO) (Patel et al., 2014), Enriched HHO (EHHO) (Chen et al., 2020), Springy whale optimization algorithm (SWOA) (Pourmousa et al., 2021). Although heuristic methods have shown better accuracy and performance than deterministic methods (Khanna et al., 2015; Kler et al., 2019; Song et al., 2021), some of these methods require a noticeably high number of iterations to converge, or different results are obtained by repeating the method. To reduce the number of iterations, and obtain consistent results as well, some improved methods have methods proposed, some of which are: Chaos Particle Swarm Optimization (CPSO) (Wei et al., 2011), Mutated Particle Swarm Optimization (MPSO) (Merchaoui et al., 2018), Guaranteed Convergence Particle Swarm Optimization (GCPSO) (Nunes et al., 2018), Improved Opposition-based whale Optimization (IOWO) (Abd Elaziz and Oliva, 2018). The root mean squared error (RMSE)-based objective function requires some experimental data from PV cells/modules that the manufacturers do not provide. Therefore, some articles selected/defined another objective function based on the information provided in the PV datasheet and identified its unknown

parameters by heuristic methods (Qais et al., 2020). Some examples are: Shuffle-Frog Leaped Optimization (Hasanien, 2015b), Bacterial Foraged Optimization (Rajasekar et al., 2013; Subudhi and Pradhan, 2017), Differential Evolution (DE) (Biswas et al., 2019; Chin et al., 2016). According to the No-Free Lunch (NFL) theorem, an optimizer cannot obtain the best global solution to all optimization problems (Wolpert and Macready, 1997). Therefore, researchers apply several optimization methods to identify/estimate the unknown parameters of the PV model.

Recently, a new metaheuristic method, called Harris Hawks optimization (HHO) algorithm, has been presented by the researchers in Heidari et al. (2019). In this algorithm, a group of hawks works together to chase a prey, and simultaneously attack the identified prey from different directions. In each stage, hawks are considered as candidate solutions and the prey is considered as the best candidate solution (optimal point). Harris hawks can deploy different chasing strategies depending on the dynamic nature of the prey's position and escaping pattern. The HHO algorithm imitates these dynamic patterns (applied by Harris Hawks to hunt the prey) to solve an optimization problem. This algorithm has been used in Aleem et al. (2019), Jia et al. (2019) and Bao et al. (2019) and showed an acceptable performance in solving different optimization problems.

Although the HHO algorithm has a good convergence speed, it gets stuck in local minima for complex optimization problems. For the problem of PV parameter identification, this issue manifests itself better once the number of unknown parameters increases. In this paper, to improve the performance of the HHO algorithm in finding the global optimum solution, an improved version, naming Whippy HHO (WHHO), has been proposed. In the proposed algorithm, modifications are applied to the process of hawks' movement towards the prey. The applied changes reduce the likelihood of getting stuck in local minima and increase the convergence speed compared to the original HHO.

In order to evaluate the performance of the proposed algorithm, first, the parameters of PV systems are identified for the SDM, DDM, TDM, and various module models as well, and the results are compared with those obtained by other well-known algorithms (both newly presented algorithms and powerful classical algorithms, such as GA and PSO). Then, to investigate the practical application of the WHHO algorithm, it was used to estimate the parameters of three types of commercial modules, i.e., polycrystalline (SW255), multi-crystalline (KC200GT), and monocrystalline (SM55), considering the effect of temperature and irradiance changes. Finally, we investigated the effect of the temperature and irradiance conditions on the value of the model parameters, as a result of which it was observed that temperature and irradiance changes yielded a change in the diode saturation current and the photo-current, respectively, and the rest of the parameters remained constant. The obtained results confirm the high performance and convergence speed of the proposed algorithm.

Other sections of the paper are organized as follows. In Section 2, the model of the PV cell and module along with the corresponding relationships are presented. In Section 3, the proposed algorithm is presented and formulated. Section 4 presents the simulations and analyzes the results. Finally, the concluding remarks are stated in Section 5.

2. Problems formulation

As mentioned in the previous section, according to the literature, several mathematical models have been proposed to simulate the behavior of PV cells and modules, among which the diode-based model is widely utilized. The reason behind using diodes in the PV equivalent circuit is that PV cell is made of

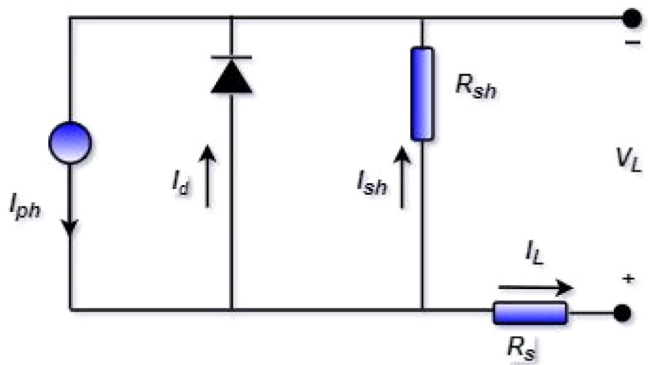


Fig. 1. Equivalent circuit of single-diode model

semiconductor materials, whose I-V characteristic exhibits exponential behavior similar to the I-V curve of a diode (Ebrahimi et al., 2019b). Each diode-based model has a number of unknown parameters (in the equivalent circuit) that must be accurately identified. In the control process of the PV system, accurate estimation of unknown parameters is very important because the value of PV model parameters presented in the datasheet will change over time due to the non-linear nature of solar cells and their aging as well (Al-Hamadi, 2015).

2.1. Single-diode model (SDM)

The single diode model (SDM) is widely used due to its simplicity. The equivalent circuit of the single diode model is shown in Fig. 1. This model includes the following elements: (1) a current source that depends on the characteristics of the semiconductor material, changes in solar irradiance, and cell/module temperature; (2) a diode that is parallel to the current source, and takes into account the physical effects in the p-n junction; (3) a series resistor (R_s) and a shunt resistor (R_{sh}) that model ohmic losses in the semiconductor and leakage current, respectively (Nunes et al., 2018; Cubas et al., 2014). The SDM is constructed based on the combination of diode's diffusion and recombination currents with defining a non-physical factor for diode ideality (AlRashidi et al., 2012)

According to the equivalent circuit, the output current (I_L) may be written as follows (Oliva et al., 2017):

$$I_L = I_{ph} - I_d - I_{sh} \quad (1)$$

The current of shunt resistance (I_{sh}) is calculated using the following equation:

$$I_{sh} = \frac{V_L + I_L R_s}{R_{sh}} \quad (2)$$

Diode current (I_d) is obtained using the Shockley equation:

$$I_d = I_{SD} \left[\exp \left(\frac{q(V_L + I_L R_s)}{nkT} \right) - 1 \right] \quad (3)$$

where k is the Boltzmann constant, q represents the electric charge, I_{SD} represents the reverse saturation (bias) current of the diode, n is the ideality factor of the diode, and T is the absolute temperature of the p-n junction, which here is the cell temperature, in Kelvin.

Finally, Eq. (1) can be rewritten using Eqs. (2) and (3):

$$I_L = I_{ph} - I_{SD} \left[\exp \left(\frac{q(V_L + I_L R_s)}{nkT} \right) - 1 \right] - \frac{V_L + I_L R_s}{R_{sh}} \quad (4)$$

Therefore, the SDM has 5 unknown parameters $\theta = [I_{ph} \ R_s \ R_{sh} \ I_{SD} \ n]$ that can be estimated.

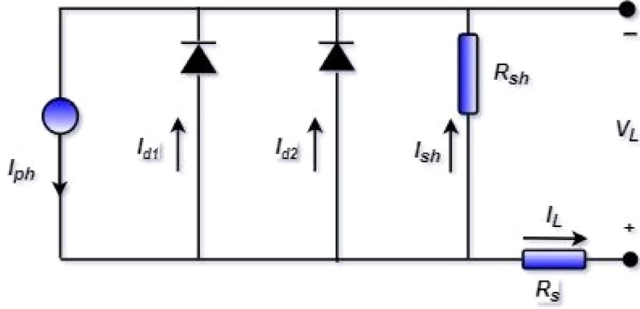


Fig. 2. Equivalent circuit of double-diode model.

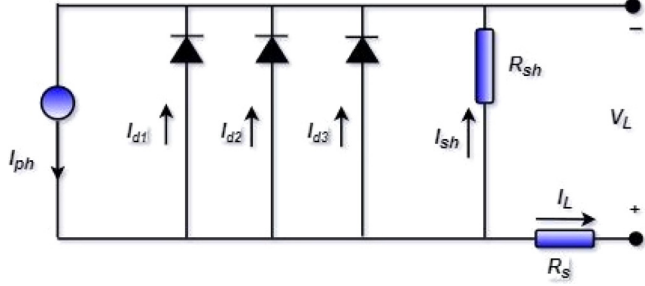


Fig. 3. Equivalent circuit of three-diode model.

2.2. Double-diode model (DDM)

The double-diode model (DDM) consists of two diodes in parallel to the current source, which more accurately describes the physical effects of the p-n junction, especially at the low level of irradiance. In fact, one diode models the diffusion current in the junction and the other diode represents the recombination effects in the space-charge region (Nunes et al., 2018). The DDM equivalent circuit is shown in Fig. 2, where I_{SD1} and I_{SD2} represent the diffusion and saturation currents, respectively, and n_1 and n_2 are the ideality factors of diffusion and recombination for the diodes, respectively.

According to the equivalent circuit of DDM, the output current is written as follows:

$$I_L = I_{ph} - I_{d1} - I_{d2} - I_{sh} \quad (5)$$

By rewriting the above equation using the same procedure presented for SDM, Eq. (6) is obtained:

$$\begin{aligned} I_L &= I_{ph} - I_{SD1} \left[\exp \left(\frac{q(V_L + I_L R_s)}{n_1 kT} \right) - 1 \right] \\ &\quad - I_{SD2} \left[\exp \left(\frac{q(V_L + I_L R_s)}{n_2 kT} \right) - 1 \right] - \frac{V_L + I_L R_s}{R_{sh}} \end{aligned} \quad (6)$$

Therefore, this model has 7 unknown parameters whose vector of unknown parameters can be defined as $\theta = [I_{ph} \ R_s \ R_{sh} \ I_{SD1} \ I_{SD2} \ n_1 \ n_2]$.

2.3. Three-diode model (TDM)

The three-diode model (TDM) is more accurate than the previous two models due to considering the effects of leakage current and grain boundaries; this consequently introduces more complexity to the model (Diab et al., 2020). As shown in Fig. 3, in this model, 3 diodes are considered in parallel to the current source.

According to the equivalent circuit, the output current relationship can be written as follows:

$$I_L = I_{ph} - I_{d1} - I_{d2} - I_{d3} - I_{sh} \quad (7)$$

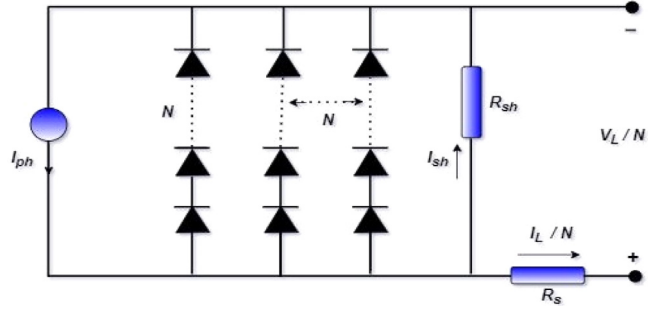


Fig. 4. Equivalent circuit of PV module model.

Using the same procedure presented in Section 2.1, Eq. (7) can be rewritten and finally, Eq. (8) is obtained:

$$\begin{aligned} I_L &= I_{ph} - I_{SD1} \left[\exp \left(\frac{q(V_L + I_L R_s)}{n_1 kT} \right) - 1 \right] \\ &\quad - I_{SD2} \left[\exp \left(\frac{q(V_L + I_L R_s)}{n_2 kT} \right) - 1 \right] \\ &\quad - I_{SD3} \left[\exp \left(\frac{q(V_L + I_L R_s)}{n_3 kT} \right) - 1 \right] - \frac{V_L + I_L R_s}{R_{sh}} \end{aligned} \quad (8)$$

Therefore, by adding the third diode, two more unknown parameters are added to the problem, and the vector of unknown parameters with 9 elements can be defined as $\theta = [I_{ph} \ R_s \ R_{sh} \ I_{SD1} \ I_{SD2} \ I_{SD3} \ n_1 \ n_2 \ n_3]$.

2.4. PV module model

As shown in Fig. 4, the PV module consists of N solar cells that are placed in series or in parallel to generate a specific amount of voltage and current. The model of these solar cells is usually considered as SDM so that they are connected in series. It is assumed that all cells are exactly the same and generate the same voltage; thus, the panel voltage will be NV_L (Ebrahimi et al., 2019b; Diab et al., 2020).

The output current of the panel (PV module) is obtained using the following relation:

$$I_L = I_{ph} - I_{SD} \times \left[\exp \left(\frac{q(V_L + NI_L R_s)}{nkTN} \right) - 1 \right] - \frac{V_L + NI_L R_s}{NR_{sh}} \quad (9)$$

where N represents the number of cells used in the PV panel.

Note that each model has a number of unknown parameters that must be carefully extracted. To evaluate the accuracy of the estimated parameters, a criterion, called the current relative error, is defined using the following equation:

$$R_{err} = \frac{I_L - I_{te}}{I_{te}} \quad (10)$$

where I_{te} is the estimated current. Smaller values of the current relative error demonstrate that the parameters have been estimated more accurately.

2.5. Objective function

To identify the unknown parameters of the PV cell/module model, an optimization problem is defined that can be solved by metaheuristic methods. By solving this optimization problem, unknown parameters are obtained in a way that the defined objective function is minimized. The objective function is usually defined based on the error between the measured current and the obtained (computed) current which has to be minimized during

the optimization process. In this article, we use the Root-Mean-Square-Error (RMSE) formulation to define the objective function, which is widely utilized in this field. The formulation of this objective function is presented in Eq. (11).

$$F(\theta) = \text{RMSE}(\theta) = \sqrt{\frac{1}{N_E} \sum_{i=1}^{N_E} f_M(V_L, I_L, \theta)^2} \quad (11)$$

In this equation, θ represents the vector of unknown parameters, N_E is the number of measured data, and M represents the type of PV model, which are single-diode (SD), double-diode (DD), three-diode (TD), panel model. f_M is also the error function, which is defined for different PV models as follows:

$$f_{SD}(V_L, I_L, \theta) = \theta_1 - \theta_4 \times \left[\exp\left(\frac{q(V_L + I_L \theta_2)}{\theta_5 kT}\right) - 1 \right] - \frac{V_L + I_L \theta_2}{\theta_3} - I_L \quad (12)$$

$$f_{DD}(V_L, I_L, \theta) = \theta_1 - \theta_4 \times \left[\exp\left(\frac{q(V_L + I_L \theta_2)}{\theta_6 kT}\right) - 1 \right] - \theta_5 \times \left[\exp\left(\frac{q(V_L + I_L \theta_2)}{\theta_7 kT}\right) - 1 \right] - \frac{V_L + I_L \theta_2}{\theta_3} - I_L \quad (13)$$

$$f_{TD}(V_L, I_L, \theta) = \theta_1 - \theta_4 \times \left[\exp\left(\frac{q(V_L + I_L \theta_2)}{\theta_7 kT}\right) - 1 \right] - \theta_5 \times \left[\exp\left(\frac{q(V_L + I_L \theta_2)}{\theta_8 kT}\right) - 1 \right] - \theta_6 \times \left[\exp\left(\frac{q(V_L + I_L \theta_2)}{\theta_9 kT}\right) - 1 \right] - \frac{V_L + I_L \theta_2}{\theta_3} - I_L \quad (14)$$

$$f_{Panel}(V_L, I_L, \theta) = \theta_1 - \theta_4 \times \left[\exp\left(\frac{q(V_L + NI_L \theta_2)}{\theta_5 kTN}\right) - 1 \right] - \frac{V_L + NI_L \theta_2}{N\theta_3} - I_L \quad (15)$$

It should be mentioned that $\theta = [\theta_1 \ \theta_2 \ \theta_3 \ \theta_4 \ \theta_5]$ is the vector of unknown parameters of SDM and PV panel/module model, $\theta = [\theta_1 \ \theta_2 \ \theta_3 \ \theta_4 \ \theta_5 \ \theta_6 \ \theta_7]$ is that of DDM, and $\theta = [\theta_1 \ \theta_2 \ \theta_3 \ \theta_4 \ \theta_5 \ \theta_6 \ \theta_7 \ \theta_8 \ \theta_9]$ is that of TDM.

3. Proposed algorithm

In this section, first, the Harris Hawks Optimization (HHO) algorithm and its formulation is discussed, and then the proposed modified version of HHO, naming whippy HHO (WHHO) is presented.

3.1. Harris Hawks optimization (HHO) algorithm

The HHO algorithm is a metaheuristic method whose stages are inspired by the behavior and chasing strategy of Harris hawks in nature. In this method, several hawks work together to attack the prey from different directions so that they simultaneously converge towards the prey they have identified. Harris hawks apply a variety of chasing strategies depending on the dynamic nature of the prey's situations and their escaping patterns (Heidari et al., 2019).

In the HHO algorithm, Harris hawks are considered as the candidate solutions and the prey is considered as the best candidate solution (or optimal solution) at each stage. At first, hawks are randomly distributed in different regions of the search space. They then identify the prey's position based on two strategies: in the first strategy, the hawks determine their new position

based on the position of other group members (other hawks) and the position of the prey; and in the second strategy, the hawks randomly determine their new position within the range the group members move. These two strategies can be mathematically defined as follows (Heidari et al., 2019):

$$\vec{X}(t+1) = \begin{cases} X_{rand}(t) - r_1 |X_{rand} - 2r_2 X(t)| & q \geq 0.5 \\ (X_{prey}(t) - X_m(t)) - r_3 (LB + r_4 (UB - LB)) & q < 0.5 \end{cases} \quad (16)$$

where $\vec{X}(t+1)$ is the hawks' position vector in the next iteration; $X_{prey}(t)$ is the prey's position in the current iteration; the coefficients r_1 , r_2 , r_3 , r_4 , and q are randomly generated numbers in the range (0,1), which are updated in each iteration; and LB and UB show the lower and upper limits of the variables, respectively. $X_{rand}(t)$ is the position of a hawk randomly selected from the current population, and $X_m(t)$ is the average position of the current population of the hawks, which can be obtained from the following equation:

$$X_m(t) = \frac{1}{W} \sum_{i=1}^W X_i(t) \quad (17)$$

where W represents the total number of hawks.

The hunting strategy of the Harris hawks is in a way that the prey gets tired and its energy decreases. The hawks then exhibit different chasing behaviors based on the prey's residual energy. The residual energy of the prey is obtained from the following equation:

$$E = 2E_0 \left(1 - \frac{t}{T}\right) \quad (18)$$

where T is the maximum number of iterations of the algorithm; and the value of E_0 in each iteration is randomly selected from the interval of (-1, +1).

In HHO algorithm, according to the amount of prey's energy (E) and escaping probability (r), four chasing strategies are utilized, each of which is described as follows.

Strategy 1: Soft besiege

When $|E|$ and r is greater than 0.5, the hawks softly encircle the prey to make it more tired, and then accomplish a surprise pounce. This behavior is modeled using the following equations (Heidari et al., 2019):

$$X(t+1) = \Delta X(t) - E |JX_{prey}(t) - X(t)| \quad (19)$$

$$\Delta X(t) = X_{prey}(t) - X(t) \quad (20)$$

where $J = 2(1 - r_5)$ represents the strength of the random jump of the escaping prey; and r_5 represents a random number in the range (0,1).

Strategy 2: Hard besiege

When $|E| < 0.5$ and $r \geq 0.5$, the prey is tired enough and the hawks strictly encircle the rabbit to make a surprise pounce. This strategy is modeled according to the following equation (Heidari et al., 2019):

$$X(t+1) = X_{prey}(t) - E |\Delta X(t)| \quad (21)$$

Strategy 3: Soft besiege with rapid leapfrogs

When $|E| \geq 0.5$ and $r < 0.5$, the prey has enough energy to perform leapfrog movements and succeed to escape. In this strategy, the concept of optimal levy flight (LF) is used to model the actual zigzag motion of the prey (Heidari et al., 2019). Therefore, the hawks can update their movement based on the following equations:

$$Y = X_{prey}(t) - E |JX_{prey}(t) - X(t)| \quad (22)$$

$$Z = Y + S * LF(D) \quad (23)$$

where D is the dimension of the problem; S is a random vector with the dimension of $(1 \times D)$; and the levy flight function is computed using the following equation:

$$LF(x) = 0.01 \times \frac{u \times \sigma}{v^{\frac{1}{\beta}}}, \sigma = \left(\frac{\Gamma(1 + \beta) \times \sin(\frac{\pi\beta}{2})}{\Gamma(\frac{1+\beta}{2}) \times \beta \times 2^{(\frac{\beta-1}{2})}} \right)^{\frac{1}{\beta}} \quad (24)$$

where v and u are random numbers in the interval of $(0, 1)$; and β is set to a constant value of 1.5. In this strategy, the position of the hawks is updated by the following equation (Heidari et al., 2019):

$$X(t+1) = \begin{cases} Y & \text{if } F(Y) < F(X(t)) \\ Z & \text{if } F(Z) < F(X(t)) \end{cases} \quad (25)$$

Strategy 4: Hard besiege with rapid leapfrogs

When $|E| < 0.5$ and $r < 0.5$, the prey is unable to escape successfully and the hawks try to reduce their average distance from the prey. This strategy can be formulated as follows (Heidari et al., 2019):

$$X(t+1) = \begin{cases} X_{rabbit}(t) - E |X_{rabbit}(t) - X_m(t)| & \text{if } F(Y) < F(X(t)) \\ Y + S * LF(D) & \text{if } F(Z) < F(X(t)) \end{cases} \quad (26)$$

3.2. Whippy HHO (WHHO)

Although the HHO algorithm has a high rate of convergence, it suffers from the issue of getting stuck in local optima, and does not converge to the global optimal solution in most cases. In the problem of parameters identification, this issue with HHO manifests itself considerably when the number of unknown parameters gets larger. In this paper, a modified version of HHO, called WHHO, is proposed to improve the performance of the original algorithm in finding the global optimum. For this purpose, the changes are applied to the process of the hawks' movement towards the desired prey (solution). To implement the changes, an elimination period has been added to the classical HHO algorithm; during each period, a certain number of the worst solutions are eliminated and replaced by the new solutions in the search space. Generating new populations allows hawks to find new trajectories to converge to the best global solution. Applying these changes to the original algorithm, the probability of getting stuck in the local optima decreases, and the speed of finding the global optimal solutions increases.

It is important to note that in the initialization step, the two parameters of the maximum number of iterations, including ep (elimination period) and et (elimination percent) are added to the classical algorithm. The former is determined based on the number of iterations T and the latter is determined based on a percentage of the initial population. (Th) Percentage of the maximum or minimum of the search space. For example, $Th = 95$, and the initial search space for the parameters is in the interval $[-1, 1]$. In each elimination phase, the value of each parameter in the particle is checked, and if it is greater than 95% of the absolute value of the search space, then one unit adds to the search space of that parameter. The steps for implementing the WHHO algorithm are shown in Fig. 5. In this figure, the steps added to the classical HHO algorithm are depicted in blue blocks.

Fig. 6 demonstrates a general overview for the estimation of parameters of the PV models using the proposed WHHO algorithm. As seen, in each iteration of the algorithm, the errors between the measured currents and the estimated currents are

calculated and then, the RMSE value is computed using Eq. (11). The objective of the WWHO algorithm is to minimize the amount of the obtained RMSE. To realize this goal, it explores the search space for the best estimate of the unknown parameters of the PV cell/module models.

4. Simulation

In this section, in order to evaluate the performance of the proposed WWHO algorithm, first, the parameters of the PV cell models (SDM, DDM, and TDM) and PV module models are identified. Voltage-current experimental data have been chosen from Ebrahimi et al. (2019b) and Yu et al. (2019) as the benchmark data, which has been widely used in the literature to assess various methods. This experimental data was extracted from a commercial silicon solar cell (R.T.C. company in France) with a diameter of 57 mm, under 1 sun (1000 W/m^2) at the temperature of 33°C , and from a commercial PV module, called Photowatt-PWP201, with 36 polycrystalline-type solar cells under 1 sun (1000 W/m^2) at the temperature of 45°C . Then, the parameters of three types of widely used modules, i.e., polycrystalline (SW255), multi-crystalline (KC200GT), and monocrystalline (SM55), under different irradiance and temperature conditions have been identified. To evaluate the accuracy of the parameters identified in the standard irradiance and temperature ($T_{STC} = 25^\circ\text{C}$, $G_{STC} = 1000 \text{ W/m}^2$), the behavior of the modules under different levels of irradiance and temperature has been investigated, as a result of which it was observed that the obtained characteristic is similar to that of the datasheet of the relevant module with an acceptable error (Ishaque et al., 2011a; Chaibi et al., 2018). Moreover, the results obtained by the proposed method are compared with those obtained by several efficient and powerful methods mentioned in Section 1. The simulations were performed in MATLAB 2016b.

In order to ensure that the search space of all problems is the same, the ranges associated with each parameter are maintained similar to what have been defined in the previous literature. Table 1 shows the ranges for each parameter of the PV cell/module model (Yu et al., 2019).

In this paper, for a more comprehensive comparison, the algorithms used in each section are different. The parameters of each algorithm are set according to the corresponding reference, except the number of iterations and the number of populations, which are considered 5000 and 30, respectively.

4.1. Parameters identification of R.T.C France solar cell

Table 2 presents the results for estimating 5 parameters of the SDM, obtained by WWHO and 9 other algorithms, including enhanced Harris Hawks Optimization (Jiao et al., 2020), performance-guided JAYA (PGJAYA) (Yu et al., 2019), flexible particle swarm optimization (FPSO) (Ebrahimi et al., 2019b), improved JAYA (IJAYA) (Yu et al., 2017), Bird Mating Optimizer (Ebrahimi et al., 2019b), generalized oppositional teaching-learning based optimization (GOTLBO) (Chen et al., 2016), Artificial bee swarm optimization (ABSO) (Askarzadeh and Rezazadeh, 2013a), genetic algorithm (GA) (AlRashidi et al., 2011), and particle swarm optimization algorithm (PSO) (Rajasekar et al., 2013). Since no information is available for the exact values of the parameters, the RMSE value is utilized as an indicator to assess the accuracy of the estimated parameters. According to the RMSE results, WWHO algorithm similar to the EHHO, FPSO, and PGJAYA methods were able to reach the lowest RMSE value, while GA reached the highest RMSE value.

Tables 3 and 4 presents the results of estimation of 7 parameters for the DDM and 9 parameters for the TDM obtained

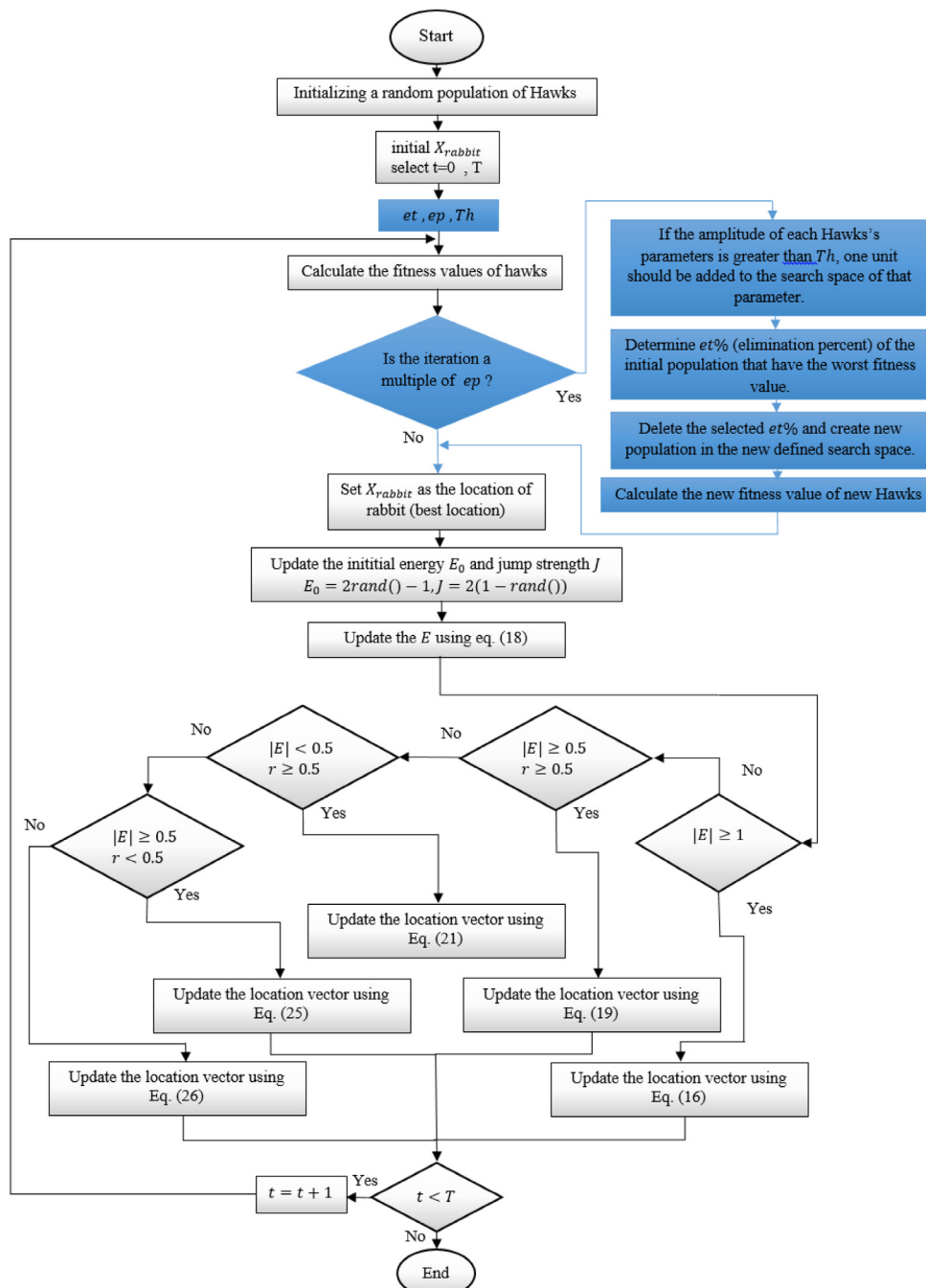


Fig. 5. Flowchart of the WWHO algorithm. (For interpretation of the references to color in this figure legend, the reader is referred to the web version of this article.)

Table 1
Parameters ranges of RTC France PV cell and PV module (Yu et al., 2019).

Parameter	RTC France PV		PWP201		PV module	
	Lower bound	Upper bound	Lower bound	Upper bound	Lower bound	Upper bound
I_{ph} (A)	0	1	0	2	0	$2I_{SC}$
I_{sd}, I_{sd2}, I_{sd3} (μ A)	0	1	0	50	0	100
R_s (Ω)	0	0.5	0	2	0	2
R_{sh} (Ω)	0	100	0	1000	0	5000
n_1, n_2	1	2	1	50	1	4
n_3	2	5	1	50		

by WWHO and 9 other algorithms, respectively. As can be observed, the proposed algorithm was able to achieve a better RMSE value compared to other algorithms for both models. Moreover,

according to results given in these tables, two remarks can be concluded: (1) TDM is a more accurate model to represent the operation of the R.T.C. FRANCE cell because most of the methods

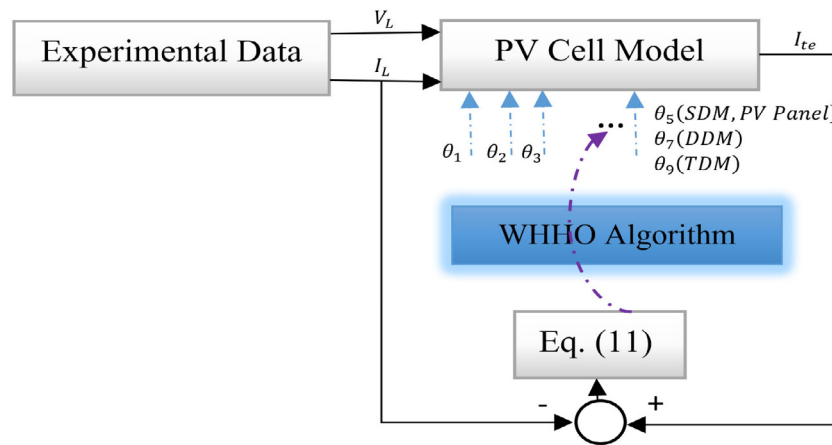


Fig. 6. A general overview of parameters estimation of PV models using WWHO algorithm.

Table 2
Detailed results for SDM of RTC France.

Algorithm	I_{ph} (A)	I_{sd1} (μ A)	R_s (Ω)	R_{sh} (Ω)	n_1	RMSE
WWHO	0.76077551	0.32302031	0.03637710	53.71867407	1.48110808	9.8602e-04
EHHO	0.760775	0.323	0.036375	53.74282	1.481238	9.8602e-04
PGJAYA	0.7608	0.3230	0.0364	53.7185	1.4812	9.8602e-04
FPSO	0.7607	0.3230	0.03637	53.7185	1.4811	9.8602e-04
IJAYA	0.7608	0.3228	0.0364	53.7595	1.4811	9.8603e-04
BMO	0.7607	0.3247	0.0363	53.8716	1.4817	9.8608e-04
GOTLBO	0.7608	0.3297	0.0363	53.3664	1.4833	9.8856e-04
ABSO	0.76080	0.30623	0.03659	52.2903	1.47583	9.9124e-04
PSO	0.7607	0.400	0.0354	59.012	1.5033	1.38e-03
GA	0.7619	0.8087	0.0299	42.3729	1.5751	1.8704e-02

Table 3
Detailed results for DDM of RTC France.

Algorithm	I_{ph} (A)	I_{sd1} (μ A)	I_{sd2} (μ A)	R_s (Ω)	R_{sh} (Ω)	n_1	n_2	RMSE
WWHO	0.76078094	0.228574	0.727182	0.03672887	55.42643282	1.451895	2	9.82487e-04
EHHO	0.76076901	0.586184	0.240965	0.03659883	55.63943956	1.968451	1.45691040	9.83606e-04
PGJAYA	0.7608	0.21031	0.88534	0.0368	55.8135	1.4450	2.0000	9.8263e-04
FPSO	0.76078	0.22731	0.72786	0.036737	55.3923	1.45160	1.99969	9.8253e-04
IJAYA	0.7601	0.00504	0.75094	0.0376	77.8519	1.2186	1.6247	9.8293e-04
BMO	0.76078	0.21110	0.87688	0.03682	55.8081	1.44533	1.99997	9.8262e-04
GOTLBO	0.7608	0.13894	0.26209	0.0365	53.4058	1.7254	1.4658	9.8742e-04
ABSO	0.076078	0.26713	0.38191	0.03657	54.6219	1.46512	1.98152	9.8344e-04
PSO	0.7623	0.4767	0.0102	0.0325	43.1034	1.5172	2	1.6600e-03
GA	0.7608	0.0001	0.0001	0.0364	53.7185	1.3355	1.481	3.6040e-01

Table 4
Detailed results for TDM of RTC France.

Algorithm	I_{ph} (A)	I_{sd1} (μ A)	I_{sd2} (μ A)	I_{sd3} (μ A)	R_s (Ω)	R_{sh} (Ω)	n_1	n_2	n_3	RMSE
WWHO	0.76078248	0.23910895	0.43972073	0.8	0.03672493	55.64995795	1.45393749	2	2.40415974	9.80751e-04
EHHO	0.76078197	0.22854289	0.57999742	0.5861	0.03676206	55.77064030	1.45029359	2	2.39655345	9.81232e-04
PGJAYA	0.7607	0.2144	0.8059	0.1178	0.0368	55.7500	1.4464	2	2.2982	9.8234e-04
FPSO	0.7607	0.2225	0.7467	0.2353	0.0367	55.7531	1.4495	2	2.5851	9.8203e-04
IJAYA	0.7608	0.2349	0.2297	0.2297	0.0367	55.2641	1.4541	1.8695	2	9.8253e-04
BMO	0.7607	0.2258	0.7504	7.9743e-08	0.0367	55.4885	1.4509	2	2.3144	9.8248e-04
GOTLBO	0.7607	0.2238	0.7583	0.0184	0.0367	55.4743	1.4501	2	2.3191	9.8245e-04
ABSO	0.7607	0.2001	0.5014	0.2102	0.0368	55.8344	1.4414	1.9156	2	9.8466e-04
PSO	0.7607	0.2259	0.7491	0.0023	0.0367	55.47571	1.4509	2	2.3156	9.8247e-04
GA	0.7605	0.3251	0.3608	0	0.0357	58.6086	1.4843	1.9975	2.2099	1.0531e-03

reached a better RMSE value for the TDM compared to the other two models; (2) the WWHO algorithm has a better performance to identify models with more unknown parameters because it yielded a lower RMSE value for the TDM, while the other algorithms showed a weaker performance with the increase in the number of unknown parameters, reaching the RMSE values very close to those of the DDM. It should be noted that the best results of all algorithms for the TDM were obtained and reported in the

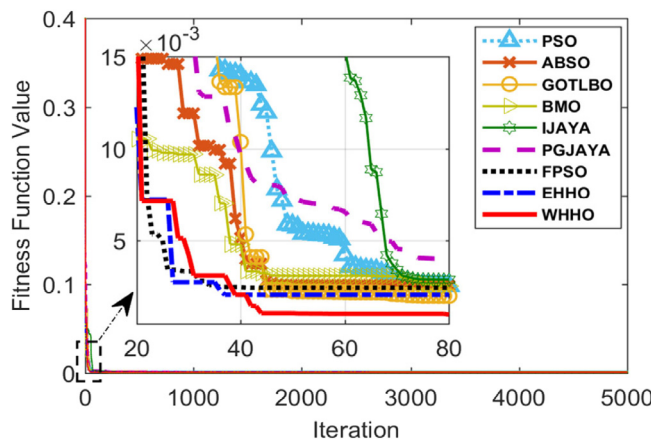
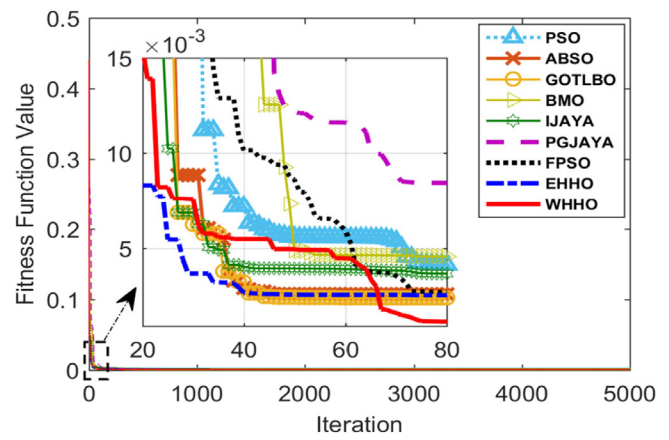
table after 30 independent runs, and they were not taken from another article.

Since all metaheuristic methods start their exploration from a random point in the search space, for a fair comparison, it is necessary that all the investigated algorithms start from the same (random) point. Furthermore, each method must be run several times so that we are able to compare the best performance of these methods with each other. **Table 5** summarizes the results

Table 5

Comparison between RMSE values for the SDM, DDM, TDM of RTC France obtained by different methods after 30 runs.

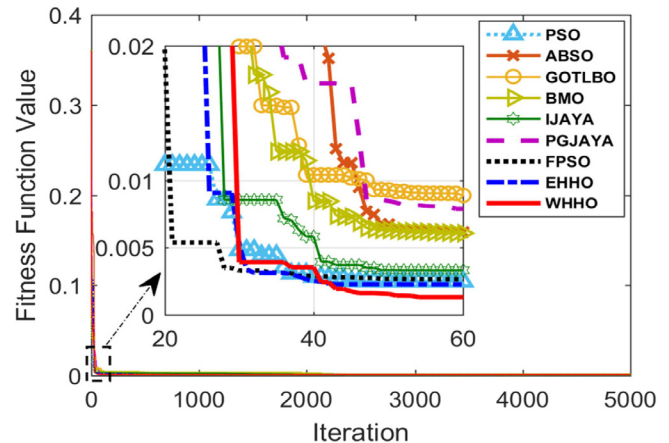
Algorithm	SDM									
	WWHO	EHHO	PGJAYA	FPSO	IJAYA	BMO	GOTLBO	ABSO	PSO	GA
Min	9.8602e-04	9.8602e-04	9.8602e-04	9.8602e-04	9.8603e-04	9.8608e-04	9.8856e-04	9.9124e-04	1.38e-03	1.8704e-02
Mean	9.8602e-04	9.8603e-03	9.8602e-04	9.8604e-04	9.9204e-04	9.8651e-04	1.0450e-03	1.10102e-03	1.3915e-03	1.9416e-02
Max	9.8602e-04	9.8603e-04	9.8603e-04	9.8652e-04	1.0622e-03	9.8701e-04	1.2067e-03	1.2013e-03	1.4512e-03	2.0136e-02
DDM										
Min	9.82487e-04	9.83606e-04	9.8263e-04	9.8253e-04	9.8293e-04	9.8262e-04	9.8742e-04	9.8344e-04	1.6600e-03	3.6040e-01
Mean	9.8249e-04	9.8401e-04	9.8582e-04	9.8330e-04	1.0296e-03	9.9156e-04	1.1475e-03	9.8781e-04	2.0891e-03	4.1297e-01
Max	9.8250e-04	9.8481e-04	9.9499e-04	9.8401e-04	1.4055e-03	9.9546e-04	1.3947e-03	9.8802e-04	2.5106e-03	1.1325e-00
TDM										
Min	9.80751e-04	9.81232e-04	9.8234e-04	9.8203e-04	9.8293e-04	9.8248e-04	9.8245e-04	9.8466e-04	9.8247e-04	1.0531e-03
Mean	9.8085e-04	9.8651e-04	9.8641e-04	9.8589e-04	9.9512e-04	2.0047e-03	9.9469e-04	9.5160e-03	2.5841e-02	1.2508e-02
Max	9.8149e-04	9.8761e-04	9.9801e-04	9.8602e-04	1.1342e-03	5.4875e-03	3.4101e-03	1.6081e-02	4.9170e-02	1.5668e-02

**Fig. 7.** RMSE evolution of the algorithms for the SDM.**Fig. 8.** RMSE evolution of the algorithms for the DDM.

of the studied algorithms obtained by 30 runs. According to the results related to the SDM, it can be seen that most of the algorithms showed a good stability and robustness. However, as the number of unknown parameters increases (for the DDM and TDM), the algorithms actually encounter a challenging problem to be optimized. Due to this challenge, the articles, proposing new algorithms, usually neglect to estimate the parameters of the TDM. As seen from Table 5, WWHO showed a very good stability for all three models compared to the other algorithms. Note that the EHHO algorithm also had a good performance in comparison with the other algorithms.

Table 6 presents the estimated current by the WWHO algorithm and the relative error for the SDM, DDM, and TDM. To ensure the accuracy of the estimated parameters, it is sufficient to investigate the relative error of the current computed using Eq. (10). As can be seen, the relative error values are very low, which indicates the accuracy of the estimated parameters. Moreover, the WWHO method was able to accurately estimate the output current of all three diode-based models.

Another factor that needs to be evaluated the convergence speed to the best solution. To show the convergence speed of the proposed algorithm, the convergence behavior of the objective function (RMSE) for the SDM, DDM, and TDM are shown in Figs. 7, 8, and 9, respectively. To ensure the high convergence speed of the WWHO, it was compared with all the algorithms presented in Table 5. As observed from these figures, the starting (randomly selected) point of all algorithms is considered to be identical so that a fair comparison can be made. According to the figures, the WWHO algorithm shows higher convergence rate than the other algorithms.

**Fig. 9.** RMSE evolution of the algorithms for the TDM.

4.2. Parameters identification of Photowatt-PWP201 PV module

In Table 7, the results for estimating 5 parameters of the SDM, obtained by WWHO and 7 other algorithms, including EHHO, JAYA (Rao, 2016), simplified teaching-learning-based optimization algorithm (STLBO) (Niu et al., 2014), teaching-learning-based artificial bee colony (TLABC) (Chen et al., 2018), comprehensive learning particle swarm optimizer (CLPSO) (Liang et al., 2006), biogeography-based learning particle swarm optimization (BLPSO) (Chen et al., 2017), and differential evolution with biogeography-based optimization (DE/BBO) (Gong et al., 2010)

Table 6
Relative error for each measurement.

DATA	V_L (V)	I_L (A)	SDM		DDM		TDM	
			I_{te} (A)	R_{err}	I_{te} (A)	R_{err}	I_{te} (A)	R_{err}
1	-0.2057	0.7640	0.764067	-0.000088	0.763986	0.000017	0.763976	0.000031
2	-0.1291	0.7620	0.762647	-0.000849	0.762605	-0.000794	0.7626	-0.000787
3	-0.0588	0.7605	0.761344	-0.001109	0.761337	-0.001100	0.761337	-0.001099
4	0.0057	0.7605	0.760148	0.000462	0.760173	0.000429	0.760177	0.000424
5	0.0646	0.7600	0.759054	0.001246	0.759106	0.001176	0.759113	0.001167
6	0.1185	0.7590	0.758044	0.001259	0.758119	0.001161	0.758128	0.001149
7	0.1678	0.7570	0.757096	-0.000127	0.757185	-0.000244	0.757194	-0.000256
8	0.2132	0.7570	0.756150	0.001123	0.756240	0.001003	0.756247	0.000994
9	0.2545	0.7555	0.755097	0.000532	0.755174	0.000430	0.755176	0.000428
10	0.2924	0.7540	0.753676	0.000428	0.753720	0.000370	0.753712	0.000380
11	0.3269	0.7505	0.751401	-0.001199	0.751395	-0.001192	0.751369	-0.001157
12	0.3585	0.7465	0.747360	-0.001151	0.747297	-0.001067	0.747238	-0.000988
13	0.3873	0.7385	0.740107	-0.002171	0.739994	-0.002019	0.739873	-0.001856
14	0.4137	0.7280	0.727403	0.000820	0.727269	0.001004	0.727033	0.001329
15	0.4373	0.7065	0.706954	-0.000642	0.706839	-0.000480	0.706413	0.000122
16	0.4590	0.6755	0.675290	0.00031	0.675232	0.000396	0.674507	0.001471
17	0.4784	0.6320	0.630875	0.001782	0.630887	0.001763	0.629750	0.003572
18	0.4960	0.5730	0.572071	0.001623	0.572138	0.001505	0.570477	0.004421
19	0.5119	0.4990	0.499480	-0.000962	0.499568	-0.001137	0.497304	0.003410
20	0.5265	0.4130	0.413485	-0.001173	0.413554	-0.001340	0.410638	0.005751
21	0.5398	0.3165	0.317214	-0.002251	0.317241	-0.002336	0.313668	0.009026
22	0.5521	0.2120	0.212101	-0.000477	0.212082	-0.000387	0.207870	0.019868
23	0.5633	0.1035	0.102722	0.007570	0.102673	0.008053	0.097869	0.057535
24	0.5736	-0.0100	-0.009246	0.081536	-0.009295	0.075762	-0.014639	-0.316930
25	0.5833	-0.1230	-0.124378	-0.011080	-0.124390	-0.011175	-0.130230	-0.055522
26	0.5900	-0.2100	-0.209190	0.003870	-0.209148	0.004072	-0.215321	-0.024716

Table 7
Detailed results for SDM of PWP201.

Algorithm	I_{ph} (A)	I_{sd1} (μ A)	R_s (Ω)	R_{sh} (Ω)	n_1	RMSE
WHHO	1.030514	3.482109e-06	1.201274	981.905230	1.349987	2.42507e-03
EHHO	1.030583	3.459968e-06	1.201853	971.276026	1.349314	2.42516e-03
JAYA	1.0307	3.4931	1.2014	1000	1.3514	2.42778e-03
STLBO	1.0305	3.4824	1.2013	982.0387	1.3511	2.42507e-03
TLMC	1.0305	3.4826	1.2013	982.1815	1.3512	2.42507e-03
CLPSO	1.0304	3.6131	1.1978	1000	1.3551	2.42806e-03
BLPSO	1.0305	3.5176	1.2002	992.7901	1.3522	2.42523e-03
DE/BBO	1.0303	3.6172	1.1969	1000	1.3552	2.42825e-03

have been presented. Again, the RMSE value is used to evaluate the accuracy of the estimated parameters. In this comparative study, the WHHO method same as the STLBO and TLMC methods could reach the lowest RMSE value.

Tables 8 and 9 show the results for estimating 7 parameters of the DDM and 9 parameters of the TDM computed by WHHO and 7 other algorithms, respectively. As observed in Table 8, the WHHO algorithm reached the lowest RMSE, while the BLPSO and CLPSO methods yielded the highest RMSE.

When the problem gets more challenging as the number of parameters increases from 7 to 9 (for the TDM), it is seen that the WHHO algorithm shows an excellent performance compared to other algorithms. Since the WHHO algorithm yielded a lower RMSE value for the TDM than the SDM and DDM, it can be concluded that the TDM is a more accurate model. It should also be noted that the best result of each algorithms for the TDM was included in Table 9 after accomplishing 30 independent runs (not taken from another article).

Since the starting point of all metaheuristic methods is randomly selected, to compare them in a fair way, several runs of each algorithm are required to be carried out. Table 10 gives the results of the studied algorithms for 30 independent runs. Based on the obtained results, it should be again noted that the proposed WHHO algorithm is an efficient algorithm in practical applications, specifically when the problem gets more complicated (for parameter identification of the TDM); in fact, it not only quickly converges to the optimal solution, but also shows a good stability and robustness.

Moving on towards parameters identification of the TDM, the complexity of the problem grows as the number of unknown parameters rises; however, as the results demonstrate, WHHO again, outperformed the other algorithms for all three diode-based models. This high performance of WHHO is due to its well-formulated capability of exploring the search space globally. Note that the EHHO method also showed a good stability for the TDM, but could not obtain the lowest RMSE value; the main reason behind this is the weakness of EHHO algorithm in performing a global search, particularly for the more complex problem.

Table 11 was made to ensure the accuracy of the estimated parameters by WHHO. This table presents the current estimated by the WHHO algorithm and the relative error (Eq. (10)) for the SDM, DDM, and TDM. As observed, the low value of the relative errors computed for WHHO confirms the accuracy of the estimated parameters, using which the output current of the SD, DD, and TD models is close to the measured values. Furthermore, WHHO led to a lower RMSE value for the TDM than the other two diode-based models. To prove this claim, we may calculate the total sum of the absolute values of the relative errors of each model separately, and it is observed that the TDM yielded a lower value of total sum than the SDM and DDM.

Moreover, as another indicator of the performance of the proposed algorithm, the convergence behavior of the fitness function (RMSE) for the SD, DD, and TD models are shown in Figs. 10, 11, and 12, respectively. We again compared WHHO with all the algorithms presented in Table 7 to perform a comprehensive investigation. As observed from these figures, the WHHO

Table 8
Detailed results for DDM of PWP201.

Algorithm	I_{ph} (A)	I_{sd1} (μ A)	I_{sd2} (μ A)	R_s (Ω)	R_{sh} (Ω)	n_1	n_2	RMSE
WHHO	1.032381	2.512910	1.000057e–06	1.239287	744.715389	1.317304	1.316937	2.046534e–03
EHHO	1.032341	2.675812	1.528211	1.233131	715.452415	1.549741	1.283921	2.2137e–03
JAYA	1.0326	2.6896	4.1973	1.2240	748.3831	1.3234	2.3680	2.2178e–03
STLBO	1.0328	2.5708	1.6899	1.2137	712.2977	1.3218	1.7314	2.2785e–03
TLABC	1.0331	2.6762	1.5280	1.2334	715.4478	1.5499	1.2832	2.2138e–03
CLPSO	1.0291	0.0010	9.3813	0.0314	75.6531	1.0000	1.5755	3.3925e–03
BLPSO	1.0265	9.2998	2.2586e–02	0.0301	1000	1.5225	1.4164	3.7559e–03
DE/BBO	1.0318	0.32774	2.4306e–06	1.2061	845.2495	1.3443	1.3443	2.400e–03

Table 9
Detailed results for TDM of PWP201.

Algorithm	I_{ph} (A)	I_{sd1} (μ A)	I_{sd2} (μ A)	I_{sd3} (μ A)	R_s (Ω)	R_{sh} (Ω)	n_1	n_2	n_3	RMSE
WHHO	1.030514	3.48214e–06	1.000010e–6	1.000000e–6	1.200216	981.869614	1.397631	1.867045	2	2.0166e–03
EHHO	1.030571	3.439412	5.361479e–5	5.365241e–3	1.210242	991.362145	1.403614	1.403715	1.598476	2.4249e–03
JAYA	1.0263	2.4380	8.4019	2.4413e–01	1.1911	710.7260	1.3885	1.8790	1.3544	2.7525e–03
STLBO	1.0327	0	5.3435	2.4748	1.1448	1000	1.8457	1.4547	1.9590	3.4186e–03
TLABC	1.0264	9.1106	2.0912e–02	6.3249e–02	1.0869	602.9147	1.5220	1.3011	1.5370	3.7258e–03
CLPSO	1.0419	3.43995	6.6266e–07	35.1499	1	755.0178	1.9938	1.2982	1.9987	9.9858e–03
BLPSO	1.0344	4.7853	1.16444	2.6812e–03	1	1000	2	1.5566	2	6.3626e–03
DE/BBO	1.0307	0	3.2036	3.1737	1.1952	996.3251	1.7749	1.3965	1.9564	2.4916e–03

Table 10
Comparison between RMSE value for the SDM, DDM, TDM of PWP201 obtained by different methods after 30 runs.

Algorithm	SDM							
	WHHO	EHHO	JAYA	STLBO	TLABC	CLPSO	BLPSO	DE/BBO
Min	2.4250e–03	2.4251e–03	2.427e–03	2.4250e–03	2.4250e–03	2.4280e–03	2.4252e–03	2.4282e–03
Mean	2.4250e–03	2.4256e–06	2.5194e–03	2.5146e–03	2.4817e–03	2.6481e–03	2.4561e–03	2.4283e–03
Max	2.4250e–03	2.4264e–03	2.8171e–03	2.7419e–03	2.6134e–03	2.7194e–03	2.5104e–03	2.4284e–03
DDM								
Min	2.0465e–03	2.2137e–03	2.2178e–03	2.2785e–03	2.2138e–03	3.3925e–03	3.7559e–03	2.400e–03
Mean	2.04816e–03	2.3651e–03	3.2472e–03	2.7113e–03	2.3147e–03	3.4461e–03	4.2541e–03	3.4618e–03
Max	2.0530e–03	2.4251e–03	3.6218e–03	2.8669e–03	2.5634e–03	3.7684e–03	4.6119e–03	4.1284e–03
TDM								
Min	2.0166e–03	2.4249e–03	2.7525e–03	3.4186e–03	3.7258e–03	9.9858e–03	6.3626e–03	2.4916e–03
Mean	2.0409e–03	2.4816e–03	3.2225e–03	3.4315e–03	4.1060e–03	1.1320e–02	9.8649e–03	1.0514e–02
Max	2.1520e–03	2.5148e–03	3.6642e–03	3.5994e–03	4.6119e–03	1.6131e–02	1.3112e–02	1.2549e–02

Table 11
Relative error for each measurement.

DATA	V_L (V)	I_L (A)	SDM		DDM		TDM	
			I_{te} (A)	R_{err}	I_{te} (A)	R_{err}	I_{te} (A)	R_{err}
1	0.1248	1.0315	1.02912247	0.00231024	1.02914861	0.00228479	1.02997462	0.00148098
2	1.8093	1.0300	1.02738460	0.00254568	1.02739312	0.00253737	1.02789154	0.00205124
3	3.3511	1.0260	1.02574227	0.00025126	1.02578124	0.00021326	1.02562143	0.00036911
4	4.7622	1.0220	1.02410401	–0.00205449	1.02410402	–0.00205449	1.02421437	–0.00216201
5	6.0538	1.0180	1.02228334	–0.00418997	1.02213478	–0.00404523	1.02215479	–0.00406473
6	7.2364	1.0155	1.01991725	–0.00433099	1.01981436	–0.00423053	1.01912247	–0.00355449
7	8.3189	1.0140	1.01635061	–0.00231280	1.01603417	–0.00200206	1.01846972	–0.00438866
8	9.3097	1.0100	1.01049121	–0.00048611	1.01045126	–0.00044659	1.01049123	–0.00048612
9	10.2163	1.0035	1.00067855	0.00281952	1.00061547	0.00288275	1.00147851	0.00201850
10	11.0449	0.9880	0.98465319	0.00339897	0.98491547	0.00313177	0.98487491	0.00317308
11	11.8018	0.9630	0.95969732	0.00344137	0.95913146	0.00403337	0.95998467	0.00314101
12	12.4929	0.9255	0.92304874	0.00265560	0.92307841	0.00262338	0.92313133	0.00256590
13	13.1231	0.8725	0.87258821	–0.00010109	0.87250148	–0.0000169	0.87297463	–0.00054369
14	13.6983	0.8075	0.80731021	0.00023508	0.80737841	0.00015059	0.80712984	0.00045861
15	14.2221	0.7265	0.72795791	–0.00200275	0.72751479	–0.00139487	0.72754631	–0.00143813
16	14.6995	0.6345	0.63646625	–0.00308933	0.63615984	–0.00260915	0.63601128	–0.00237618
17	15.1346	0.5345	0.53569611	–0.00223282	0.53521364	–0.00133337	0.53556487	–0.00198831
18	15.5311	0.4275	0.42881615	–0.00306927	0.42856947	–0.00249544	0.42881516	–0.00306696
19	15.8929	0.3185	0.31866863	–0.00052917	0.31861643	–0.00036542	0.31869794	–0.00062108
20	16.2229	0.2085	0.20785706	0.00309314	0.20791597	0.00280897	0.20789748	0.00289815
21	16.5241	0.1010	0.09835411	0.02690116	0.09891547	0.02107385	0.09899491	0.02025447
22	16.7987	–0.0080	–0.00816938	–0.02073369	–0.00815147	–0.01858192	–0.00810304	–0.01271621
23	17.0499	–0.1110	–0.11096848	0.00028402	–0.11096914	0.00027809	–0.11091012	0.00081038
24	17.2793	–0.2090	–0.20911760	–0.00056238	–0.20912547	–0.00059997	–0.20918451	–0.00088204
25	17.4885	–0.3030	–0.30202232	0.00323710	–0.30214697	0.00282322	–0.30256284	0.00144485

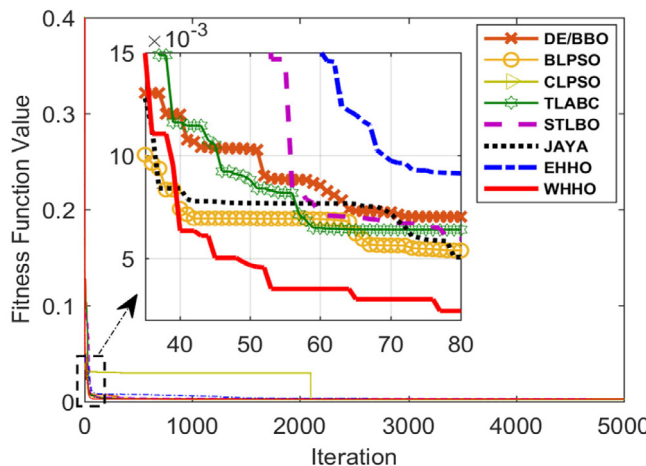


Fig. 10. RMSE evolution of the algorithms for the SDM.

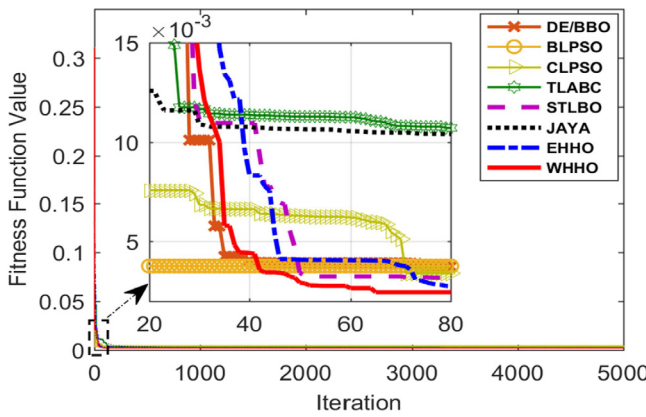


Fig. 11. RMSE evolution of the algorithms for the DDM.

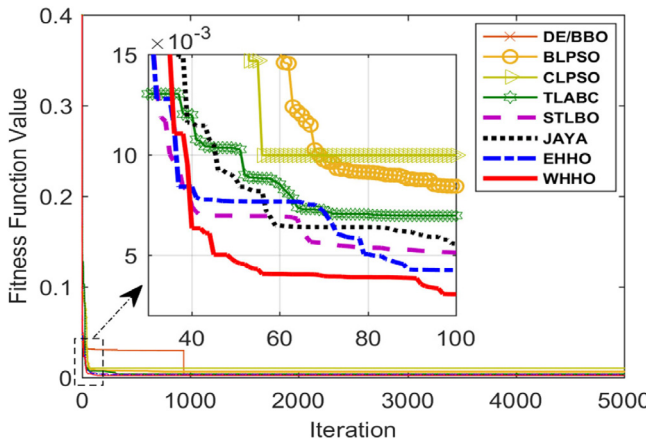


Fig. 12. RMSE evolution of the algorithms for the TDM.

method converges to the optimal solution faster than the other algorithms.

4.3. Experimental study

In this part, we investigate the variation of PV modules' I-V characteristics under changing irradiance and temperature conditions. The selected PV modules to carry out our investigation include SM55 (mono-crystalline) (Ishaque et al., 2011a), KC200GT

Table 12

Experimental data of the investigated modules under STC.

Parameters	SM55	KC200GT	SW255
Maximum power (P_{\max} (W))	55	200	255
Voltage at P_{\max} (V_{ppm} (V))	17.4	26.3	31.4
Current at P_{\max} (I_{ppm} (A))	3.15	7.61	8.15
Open circuit voltage (V_{oc} (V))	21.7	32.9	37.8
Short circuit Current (I_{sc} (A))	3.45	8.21	8.66
K_V (mV/°C)	-76	-123	-30
K_I (mA/°C)	1.40	3.18	4
Number of cells	36	54	60

Table 13

Parameters of the three PV modules identified by the WHHO method at STC.

Parameters	SM55	KC200GT	SW255
I_{ph} (A)	3.46575503	8.21860582	8.67223408
I_{sd1} (μ A)	2.26360312e-04	0.00143601	0.01620409
R_s (Ω)	0.32241761	0.24093983	0.12261139
R_{sh} (Ω)	311.82004454	774.212315	825.147321
n_1	1.0008282340	1.05528589	1.21928131
RMSE	0.02078510	0.01821364	0.01452717

(multi-crystalline) (Ishaque et al., 2011a), and SW255 (polycrystalline) (Chaibi et al., 2018) modules. Table 12 summarizes the three modules' specifications taken out from their datasheets at an irradiance of Sun = 1000 W/m², and temperature of $T = 25^\circ\text{C}$, i.e., standard test conditions (STC).

We may define a function for the PV current in terms of the temperature and irradiance using the following equation (Ishaque et al., 2011a):

$$I_{ph} = (I_{ph_STC} + K_i \Delta T) \frac{G}{G_{STC}} \quad (27)$$

where I_{ph_STC} represents the diode's photocurrent at STC (in Ampere); $\Delta T = T - T_{STC}$ which is in Kelvin; and G and G_{STC} represent the irradiance on the cell's surface and the irradiance at STC, respectively. K_i is a constant coefficient representing the short-circuit current, which is extracted from the datasheet. Eq. (28) define the saturation current in terms of the temperature change (Ishaque et al., 2011a):

$$I_{SD} = \frac{(I_{SC_STC} + K_i \Delta T)}{\exp[q(V_{OC_STC} + K_v \Delta T)/nkT] - 1} \quad (28)$$

K_v is a constant coefficient representing the open-circuit voltage, which is also provided by the manufacturer.

In this study, we have identified the PV modules' parameters by implementing the WHHO algorithm in MATLAB m-script and using the information extracted from the technical brochure. Table 13 summarizes the estimation results for the studied modules. According to the results, the proposed algorithm yielded very low RMSE values for all three investigated modules.

The I-V (current-voltage) and P-V (power-voltage) characteristics of the SM55 module for different irradiance conditions at a constant temperature $T = 25^\circ\text{C}$, and various temperatures at a constant irradiance $G = 1000 \text{ W/m}^2$ are depicted in Figs. 13 and 14, respectively.

Figs. 15 and 16 demonstrates the I-V and P-V curves of the KC 200GT module for different irradiance conditions at a constant STC temperature and various temperature values at constant STC irradiance, respectively.

The I-V and P-V curves of the SW255 module for various irradiance conditions changing in the interval between 200 W/m² and 1000 W/m² at a constant temperature of $T = 25^\circ\text{C}$ are shown in Fig. 17. It should be mentioned that the I-V characteristic of SW255 module under various temperature conditions are not provided by the manufacturer. Comparing the curves plotted

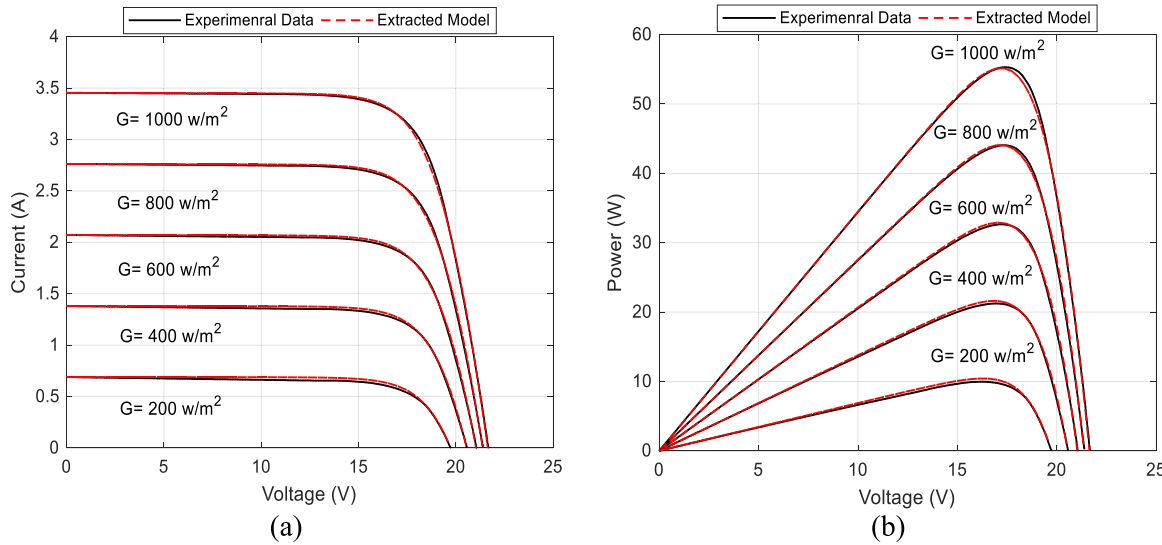


Fig. 13. Evaluation of the characteristics of SM55 module for the parameters estimated by the proposed algorithm in comparison with those provided by the manufacturer under irradiance changes at constant $T = 25^\circ\text{C}$; (a) I-V curve; (b) P-V curve.

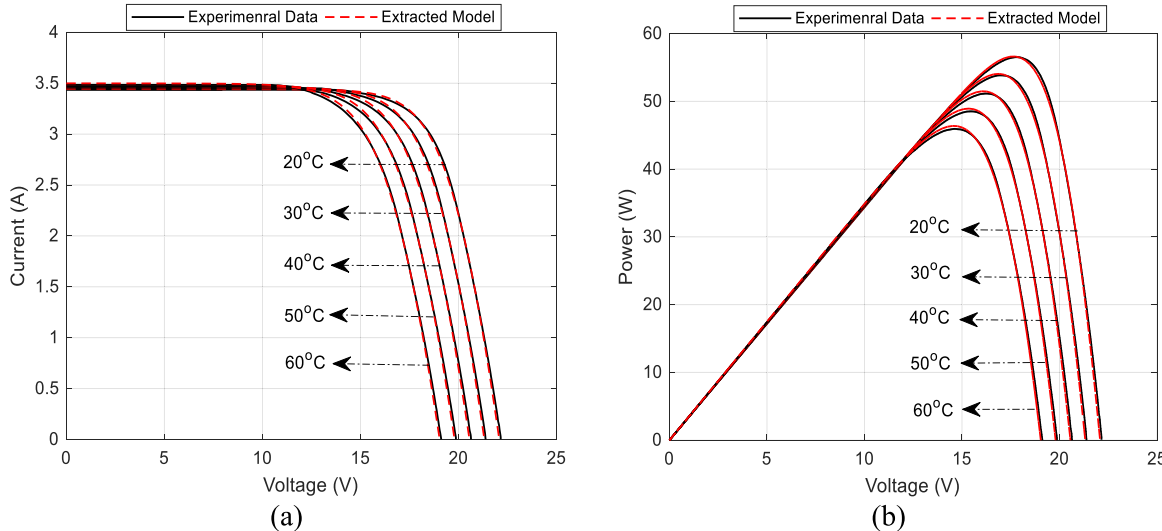


Fig. 14. Evaluation of the characteristics of SM55 module for the parameters estimated by the proposed algorithm in comparison with those provided by the manufacturer under temperature changes at constant $G = 1000 \text{ W/m}^2$; (a) I-V curve; (b) P-V curve.

using the experimental data and estimated parameters, we may explicitly observe that they are appropriately consistent for all the studied PV modules.

4.4. The effects of the temperature and irradiance on the module parameters

Table 14 presents the results obtained by WHHO for estimating 5 parameters of the SDM of the widely used SM55, KC200GT, and SW255 modules.

The inputs of the PV module model include irradiance, temperature, series resistance, and shunt resistance. The current-voltage (I-V) characteristic of PV cells depends on two factors: temperature and irradiance. The output power increases with decreasing temperature and increasing irradiance, while it decreases with increasing temperature and decreasing irradiance. In fact, output power has a direct and inverse relationship with the

irradiance and temperature, respectively. It can be seen from Tables 14 and 15 that the estimated parameters I_{ph} (A) and I_{sd1} (μA) change under different irradiance and temperature conditions, respectively. However, the series resistor R_s (Ω), shunt resistor R_{sh} (Ω), and n_1 remain almost constant under different operating conditions. From a physics point of view, I_{ph} is the photocurrent and its value increases with increasing the irradiance level, which can be seen in the results given in Table 14. The parameter I_{sd1} is the reverse saturation current of the diode and its value depends on the temperature; as the temperature increases, the photon absorption increases, and as a result, the value of I_{sd1} increases. This phenomenon has been also confirmed by the results presented in Table 15 (Zekry et al., 2018; Yu et al., 2019).

Note that the value of the series resistance R_s for Mono-crystalline and Multi-crystalline modules is less than 0.4, which is exactly in accordance with the theoretical prediction of a smaller value of the series resistance and a higher value of the shunt

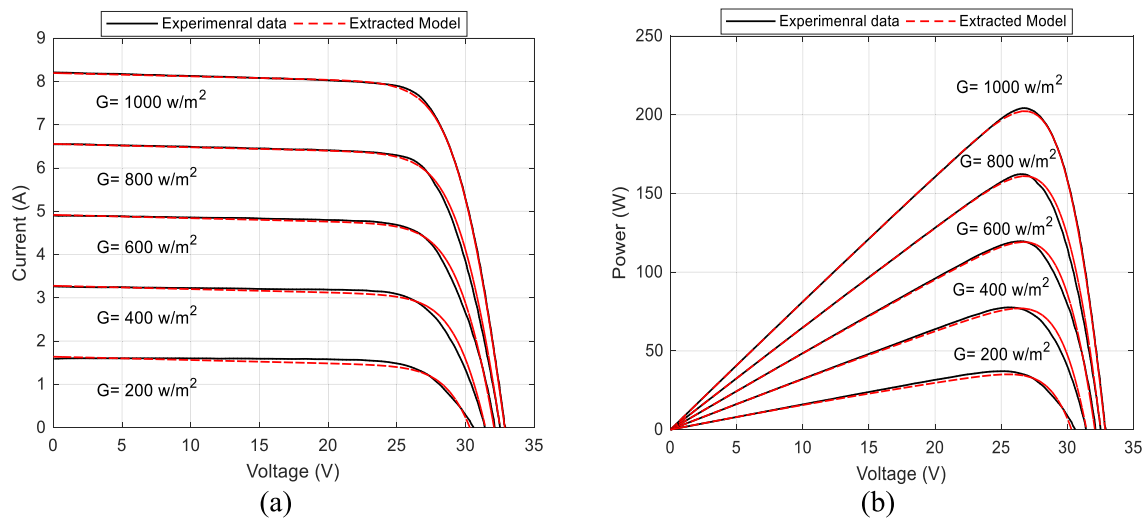


Fig. 15. Evaluation of the characteristics of KC 200GT module for the parameters estimated by the proposed algorithm in comparison with those provided by the manufacturer under irradiance changes at constant $T = 25^\circ\text{C}$; (a) I-V curve; (b) P-V curve.

Table 14

Optimal estimated parameters by WWHO for three types of PV modules at different irradiance (G) and constant temperature of 25°C .

Parameters	SM55	KC200GT	SW255
$G = 200$			
I_{ph} (A)	0.69154268	1.64591486	1.74616742
I_{sd1} (μA)	0.14641839	5.37411e-04	0.03315961
R_s (Ω)	0.28631598	0.37881647	0.38834154
R_{sh} (Ω)	449.145212	699.314567	912.314614
n_1	1.37725164	1.00469512	1.27498453
RMSE	3.21124e-04	1.40241e-03	9.93614e-03
$G = 400$			
I_{ph} (A)	1.39241561	3.28142454	3.47661479
I_{sd1} (μA)	0.10042132	1.61034e-03	0.02016954
R_s (Ω)	0.39771201	0.36311290	0.25641579
R_{sh} (Ω)	431.125419	761.215416	910.452548
n_1	1.36201547	1.05121344	1.24512479
RMSE	7.21015e-04	1.41431e-03	0.01136479
$G = 600$			
I_{ph} (A)	2.10125481	4.94215634	5.20891846
I_{sd1} (μA)	0.15612384	4.21342e-03	9.63147e-03
R_s (Ω)	0.33124562	0.31526941	0.20115943
R_{sh} (Ω)	451.231478	761.819153	923.142347
n_1	1.37167482	1.07123486	1.19194163
RMSE	8.34159e-04	1.33236e-03	0.01535849
$G = 800$			
I_{ph} (A)	2.77613912	6.5813479	6.93764791
I_{sd1} (μA)	0.14986431	9.81279e-04	0.01294763
R_s (Ω)	0.32915623	0.34261571	0.14915478
R_{sh} (Ω)	449.614515	763.158443	846.784126
n_1	1.38012141	1.05619437	1.20661473
RMSE	6.64345e-04	1.61347e-03	0.01959181
$G = 1000$			
I_{ph} (A)	3.45001264	8.21051643	8.67296365
I_{sd1} (μA)	0.17153147	2.23145e-03	0.01646397
R_s (Ω)	0.32514693	0.34157893	0.12219467
R_{sh} (Ω)	452.349781	765.351981	825.147312
n_1	1.38597463	1.06158614	1.21925646
RMSE	9.01452e-04	1.51238e-03	0.01452197

resistance. It should be also noted that the value of the ideality factor of diode n_1 is different for different types of PV models. For example, for KC200GT, its value is close to 1 because this type of PV model is a diffusion-guided device (Yu et al., 2019).

In summary, the investigations carried out in this section show that the parameters estimated by the proposed WWHO algorithm are accurate and valid under different operating conditions. It should be noted that the obtained results are in accordance with the results of the other methods (Merchaoui et al., 2018; Rajasekar et al., 2013; Ebrahimi et al., 2019a; Xu and Wang, 2017; Pourmousa et al., 2019).

5. Conclusion

In this paper, a new optimization algorithm, naming whippy Harris Hawks Optimization (WWHO), was proposed to enhance the performance of the original HHO algorithm. Some remarkable features of the proposed algorithm include high convergence speed, global exploration, and high robustness. In order to evaluate the performance of the proposed algorithm, the model parameters of PV cell and PV modules have been identified for the SDM, DDM, TDM, and module model, and the results have been compared with some other well-known and powerful methods applied in the relevant literature. Implementing various experiments, we observed that the computed results were so close to the experimental data of the modules, which confirms the high performance and accuracy of the proposed algorithm.

To investigate the performance of the WWHO algorithm in the practical application, it was used to estimate the parameters of three types of commercial modules considering the effect of temperature and irradiance changes. Finally, we studied the variation of the estimated parameters by changing the temperature and irradiance conditions. It was observed that the saturation current of the diode and the photocurrent slightly change with the variation of the temperature and irradiance, respectively, and the rest of the parameters remain almost constant under various operating conditions.

Declaration of competing interest

The authors declare that they have no known competing financial interests or personal relationships that could have appeared to influence the work reported in this paper.

Acknowledgment

Funding support from: Natural Sciences and Engineering Research Council (NSERC) of Canada, Discovery Grant # RGPIN-2017-04087 (Gadsden).

$T = 25^{\circ}\text{C}$; (a) I-V curve; (b) P-V curve.

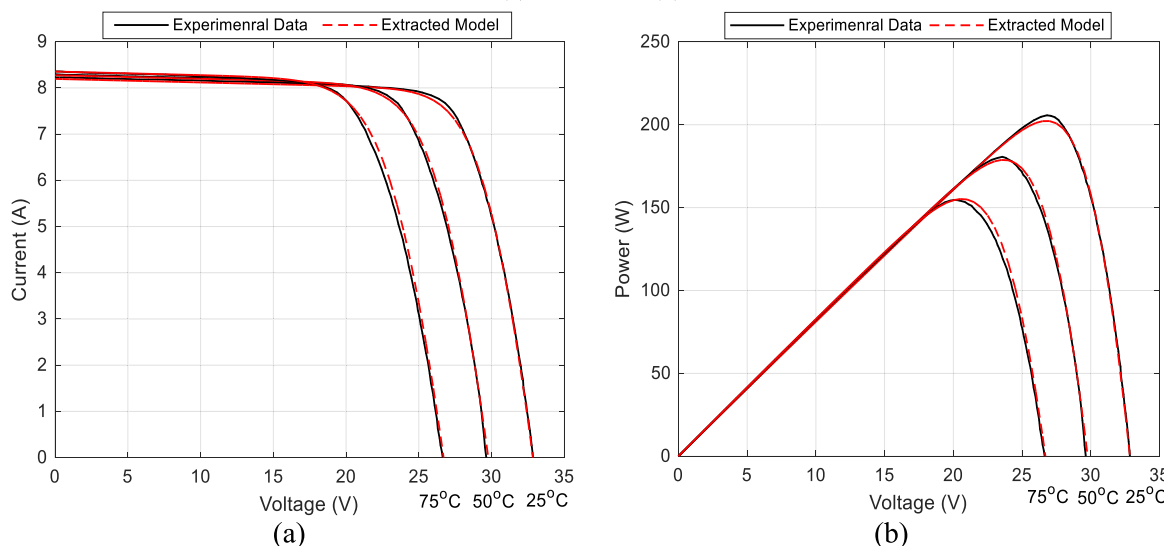


Fig. 16. Evaluation of the characteristics of KC 200GT module for the parameters estimated by the proposed algorithm in comparison with those provided by the manufacturer under temperature changes at constant irradiance $G = 1000 \text{ W/m}^2$; (a) I-V curve; (b) P-V curve.

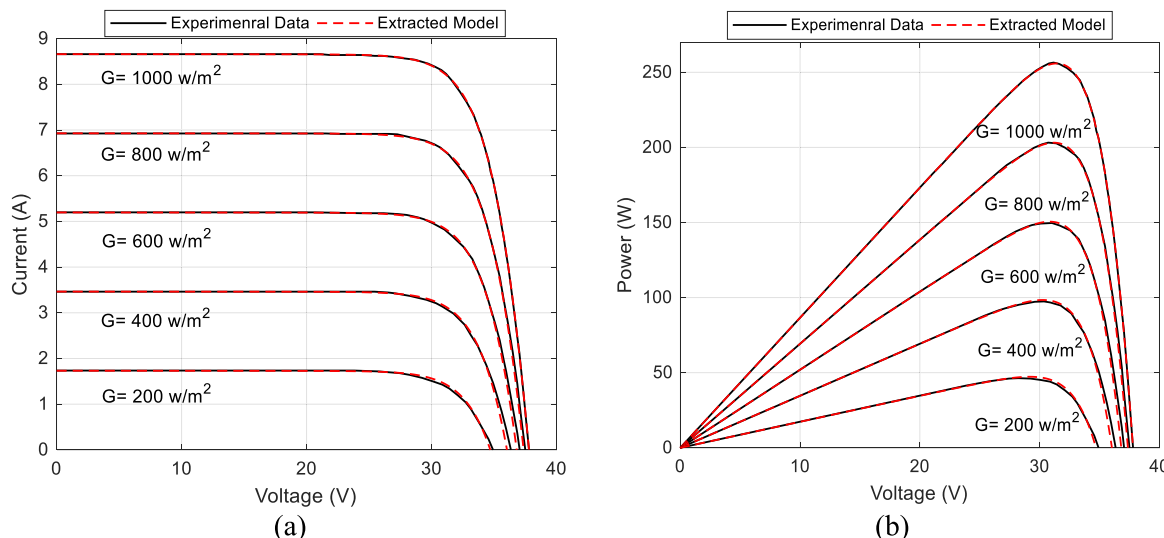


Fig. 17. Evaluation of the characteristics of SW255 module for the parameters estimated by the proposed algorithm in comparison with those provided by the manufacturer under irradiance changes at constant $T = 25^{\circ}\text{C}$; (a) I-V curve; (b) P-V curve.

Table 15

Optimal estimated parameters by WWHO for three modules at different temperature values and constant irradiance of 1000 W/m^2 .

PV Modules	Temperature	I_{ph} (A)	I_{sd1} (μA)	R_s (Ω)	R_{sh} (Ω)	n_1	RMSE
SM55	20 °C	3.43012610	0.15141237	0.32493172	458.1486	1.38416982	9.2631e-04
	30 °C	3.45167312	0.17954136	0.31647831	475.6415	1.37621438	9.0532e-04
	40 °C	3.46913647	1.06184731	0.31594137	511.3479	1.41213461	3.4263e-03
	50 °C	3.47816739	3.15948234	0.32153476	584.6174	1.38362494	3.4161e-03
	60 °C	3.49462817	6.84165721	0.32130415	498.2461	1.40346171	3.7561e-03
KC200GT	25 °C	8.21051643	2.23145e-03	0.34157893	765.3519	1.06158614	1.51238e-03
	50 °C	8.29314912	0.12638419	0.33614281	820.1674	1.08631425	2.6791e-03
	75 °C	8.37712648	1.64179431	0.33671429	806.9413	1.07641739	4.3149e-03

References

- Abbassi, R., Abbassi, A., Heidari, A.A., Mirjalili, S., 2019. An efficient salp swarm-inspired algorithm for parameters identification of photovoltaic cell models. *Energy Convers. Manage.* 179, 362–372.
- Abd Elaziz, M., Oliva, D., 2018. Parameter estimation of solar cells diode models by an improved opposition-based whale optimization algorithm. *Energy Convers. Manage.* 171, 1843–1859.
- Al-Hamadi, H., 2015. Fuzzy estimation analysis of photovoltaic model parameters. *J. Power Energy Eng.* 3 (07), 39.
- Alam, D.F., Yousri, D.A., Eteiba, M.B., 2015. Flower pollination algorithm based solar PV parameter estimation. *Energy Convers. Manage.* 101, 410–422.
- Aleem, S.H.A., Zobaa, A.F., Balci, M.E., Ismael, S.M., 2019. Harmonic overloading minimization of frequency-dependent components in harmonics polluted distribution systems using harris hawks optimization algorithm. *IEEE Access* 7, 100824–100837.

- Allam, D., Yoursri, D.A., Eteiba, M.B., 2016. Parameters extraction of the three diode model for the multi-crystalline solar cell/module using Moth-Flame Optimization Algorithm. *Energy Convers. Manage.* 123, 535–548.
- AlRashidi, M.R., AlHajri, M.F., El-Naggar, K.M., Al-Othman, A.K., 2011. A new estimation approach for determining the I-V characteristics of solar cells. *Sol. Energy* 85 (7), 1543–1550.
- AlRashidi, M.R., El-Naggar, K.M., AlHajri, M.F., 2012. Heuristic approach for estimating the solar cell parameters. In: Recent Researches in Applied Information Science, Vol. 2. pp. 80–83.
- Askarzadeh, A., Rezazadeh, A., 2012. Parameter identification for solar cell models using harmony search-based algorithms. *Sol. Energy* 86 (11), 3241–3249.
- Askarzadeh, A., Rezazadeh, A., 2013a. Artificial bee swarm optimization algorithm for parameters identification of solar cell models. *Appl. Energy* 102, 943–949.
- Askarzadeh, A., Rezazadeh, A., 2013b. Extraction of maximum power point in solar cells using bird mating optimizer-based parameters identification approach. *Sol. Energy* 90, 123–133.
- Ayang, A., Wamkeue, R., Ouhrouche, M., Djongyang, N., Salomé, N.E., Pombe, J.K., Ekemb, G., 2019. Maximum likelihood parameters estimation of single-diode model of photovoltaic generator. *Renew. Energy* 130, 111–121.
- Babu, B.C., Gurjar, S., 2014. A novel simplified two-diode model of photovoltaic (PV) module. *IEEE J. Photovolt.* 4 (4), 1156–1161.
- Bao, X., Jia, H., Lang, C., 2019. A novel hybrid harris hawks optimization for color image multilevel thresholding segmentation. *IEEE Access* 7, 76529–76546.
- Biswas, P.P., Suganthan, P.N., Wu, G., Amaralunga, G.A., 2019. Parameter estimation of solar cells using datasheet information with the application of an adaptive differential evolution algorithm. *Renew. Energy* 132, 425–438.
- Cárdenas, A.A., Carrasco, M., Mancilla-David, F., Street, A., Cárdenas, R., 2016. Experimental parameter extraction in the single-diode photovoltaic model via a reduced-space search. *IEEE Trans. Ind. Electron.* 64 (2), 1468–1476.
- Celik, A.N., Acikgoz, N., 2007. Modelling and experimental verification of the operating current of mono-crystalline photovoltaic modules using four-and five-parameter models. *Appl. Energy* 84 (1), 1–15.
- Chaibi, Y., Salhi, M., El-Jouni, A., Essadki, A., 2018. A new method to extract the equivalent circuit parameters of a photovoltaic panel. *Sol. Energy* 163, 376–386.
- Chan, D.S., Phang, J.C., 1987. Analytical methods for the extraction of solar-cell single-and double-diode model parameters from IV characteristics. *IEEE Trans. Electron Devices* 34 (2), 286–293.
- Chan, D.S.H., Phillips, J.R., Phang, J.C.H., 1986. A comparative study of extraction methods for solar cell model parameters. *Solid-State Electron.* 29 (3), 329–337.
- Chatterjee, A., Keyhani, A., Kapoor, D., 2011. Identification of photovoltaic source models. *IEEE Trans. Energy Convers.* 26 (3), 883–889.
- Chegaa, M., Ouennoughi, Z., Hoffmann, A., 2001. A new method for evaluating illuminated solar cell parameters. *Solid-State Electron.* 45 (2), 293–296.
- Chen, H., Jiao, S., Wang, M., Heidari, A.A., Zhao, X., 2020. Parameters identification of photovoltaic cells and modules using diversification-enriched Harris hawks optimization with chaotic drifts. *J. Cleaner Prod.* 244, 118778.
- Chen, X., Tianfield, H., Mei, C., Du, W., Liu, G., 2017. Biogeography-based learning particle swarm optimization. *Soft Comput.* 21 (24), 7519–7541.
- Chen, X., Xu, B., Mei, C., Ding, Y., Li, K., 2018. Teaching-learning-based artificial bee colony for solar photovoltaic parameter estimation. *Appl. Energy* 212, 1578–1588.
- Chen, X., Yu, K., Du, W., Zhao, W., Liu, G., 2016. Parameters identification of solar cell models using generalized oppositional teaching learning based optimization. *Energy* 99, 170–180.
- Chenche, L.E.P., Mendoza, O.S.H., Bandarra Filho, E.P., 2018. Comparison of four methods for parameter estimation of mono-and multi-junction photovoltaic devices using experimental data. *Renew. Sustain. Energy Rev.* 81, 2823–2838.
- Chenouard, R., El-Sehiemy, R.A., 2020. An interval branch and bound global optimization algorithm for parameter estimation of three photovoltaic models. *Energy Convers. Manage.* 205, 112400.
- Chin, V.J., Salam, Z., Ishaque, K., 2016. An accurate modelling of the two-diode model of PV module using a hybrid solution based on differential evolution. *Energy Convers. Manage.* 124, 42–50.
- Cubas, J., Pindado, S., Victoria, M., 2014. On the analytical approach for modeling photovoltaic systems behavior. *J. Power Sources* 247, 467–474.
- Derick, M., Rani, C., Rajesh, M., Farrag, M.E., Wang, Y., Busawon, K., 2017. An improved optimization technique for estimation of solar photovoltaic parameters. *Sol. Energy* 157, 116–124.
- Di Piazza, M.C., Luna, M., Petrone, G., Spagnuolo, G., 2017. Translation of the single-diode PV model parameters identified by using explicit formulas. *IEEE J. Photovolt.* 7 (4), 1009–1016.
- Diab, A.A.Z., Sultan, H.M., Aljendy, R., Al-Sumaiti, A.S., Shoyama, M., Ali, Z.M., 2020. Tree growth based optimization algorithm for parameter extraction of different models of photovoltaic cells and modules. *IEEE Access* 8, 119668–119687.
- Easwarakhanthan, T., Bottin, J., Bouhouc, I., Boutrit, C., 1986. Nonlinear minimization algorithm for determining the solar cell parameters with microcomputers. *Int. J. Sol. Energy* 4 (1), 1–12.
- Ebrahimi, S.M., Malekzadeh, M., Alizadeh, M., HosseiniNia, S.H., 2019a. Parameter identification of nonlinear system using an improved lozi map based chaotic optimization algorithm (ILCOA). *Evol. Syst.* 1–18.
- Ebrahimi, S.M., Salahshour, E., Malekzadeh, M., Gordillo, F., 2019b. Parameters identification of PV solar cells and modules using flexible particle swarm optimization algorithm. *Energy* 179, 358–372.
- El Achoubi, H., Zaimi, M., Ibral, A., Assaid, E.M., 2018. New analytical approach for modelling effects of temperature and irradiance on physical parameters of photovoltaic solar module. *Energy Convers. Manage.* 177, 258–271.
- El-Fergany, A., 2015. Efficient tool to characterize photovoltaic generating systems using mine blast algorithm. *Electr. Power Compon. Syst.* 43 (8–10), 890–901.
- El-Naggar, K.M., AlRashidi, M.R., AlHajri, M.F., Al-Othman, A.K., 2012. Simulated annealing algorithm for photovoltaic parameters identification. *Sol. Energy* 86 (1), 266–274.
- Elazab, O.S., Hasanien, H.M., Elgendy, M.A., Abdeen, A.M., 2018. Parameters estimation of single-and multiple-diode photovoltaic model using whale optimisation algorithm. *IET Renew. Power Gener.* 12 (15), 1755–1761.
- Gholipour, R., Addeh, J., Mojallali, H., Khosravi, A., 2012a. Multi-objective evolutionary optimization of PID controller by chaotic particle swarm optimization. *Int. J. Comput. Electr. Eng.* 4 (6), 833.
- Gholipour, R., Khosravi, A., Mojallali, H., 2015. Multi-objective optimal backstepping controller design for chaos control in a rod-type plasma torch system using Bees algorithm. *Appl. Math. Model.* 39 (15), 4432–4444.
- Gholipour, R., Khosravi, A., Mojallali, H., Addeh, J., 2012b. Chaos control of Iur'e like chaotic system using backstepping controller optimized by chaotic particle swarm optimization. *Int. J. Comput. Sci. Issues* 9 (2), 360–370.
- Gong, W., Cai, Z., Ling, C.X., 2010. DE/BBO: a hybrid differential evolution with biogeography-based optimization for global numerical optimization. *Soft Comput.* 15 (4), 645–665.
- Guo, L., Meng, Z., Sun, Y., Wang, L., 2016. Parameter identification and sensitivity analysis of solar cell models with cat swarm optimization algorithm. *Energy Convers. Manage.* 108, 520–528.
- Hasanien, H.M., 2015a. An adaptive control strategy for low voltage ride through capability enhancement of grid-connected photovoltaic power plants. *IEEE Trans. Power Syst.* 31 (4), 3230–3237.
- Hasanien, H.M., 2015b. Shuffled frog leaping algorithm for photovoltaic model identification. *IEEE Trans. Sustain. Energy* 6 (2), 509–515.
- Heidari, A.A., Mirjalili, S., Faris, H., Aljarah, I., Mafarja, M., Chen, H., 2019. Harris hawks optimization: Algorithm and applications. *Future Gener. Comput. Syst.* 97, 849–872.
- Hejri, M., Mokhtari, H., Azizian, M.R., Ghandhari, M., Söder, L., 2014. On the parameter extraction of a five-parameter double-diode model of photovoltaic cells and modules. *IEEE J. Photovolt.* 4 (3), 915–923.
- Ibrahim, I.A., Hossain, M.J., Duck, B.C., Nadarajah, M., 2020. An improved wind driven optimization algorithm for parameters identification of a triple-diode photovoltaic cell model. *Energy Convers. Manage.* 213, 112872.
- Imani, M.H., Niknejad, P., Barzegaran, M.R., 2018a. The impact of customers' participation level and various incentive values on implementing emergency demand response program in microgrid operation. *Int. J. Electr. Power Energy Syst.* 96, 114–125.
- Imani, M.H., Niknejad, P., Barzegaran, M.R., 2019. Implementing time-of-use demand response program in microgrid considering energy storage unit participation and different capacities of installed wind power. *Electr. Power Syst. Res.* 175, 105916.
- Imani, M.H., Yousefpour, K., Ghadi, M.J., Andani, M.T., 2018b. Simultaneous presence of wind farm and V2G in security constrained unit commitment problem considering uncertainty of wind generation. In: 2018 IEEE Texas Power and Energy Conference (TPEC). IEEE, pp. 1–6.
- Ishaque, K., Salam, Z., Taheri, H., 2011a. Modeling and simulation of photovoltaic (PV) system during partial shading based on a two-diode model. *Simul. Model. Pract. Theory* 19 (7), 1613–1626.
- Ishaque, K., Salam, Z., Taheri, H., 2011b. Simple, fast and accurate two-diode model for photovoltaic modules. *Sol. Energy Mater. Sol. Cells* 95 (2), 586–594.
- Ismail, M.S., Moghavemi, M., Mahlia, T.M.I., 2013. Characterization of PV panel and global optimization of its model parameters using genetic algorithm. *Energy Convers. Manage.* 73, 10–25.
- Jia, H., Lang, C., Oliva, D., Song, W., Peng, X., 2019. Dynamic harris hawks optimization with mutation mechanism for satellite image segmentation. *Remote Sens.* 11 (12), 1421.
- Jiao, S., Chong, G., Huang, C., Hu, H., Wang, M., Heidari, A.A., Chen, H., Zhao, X., 2020. Orthogonally adapted Harris hawks optimization for parameter estimation of photovoltaic models. *Energy* 203, 117804.
- Jordehi, A.R., 2016. Parameter estimation of solar photovoltaic (PV) cells: A review. *Renew. Sustain. Energy Rev.* 61, 354–371.
- Khanna, V., Das, B.K., Bisht, D., Singh, P.K., 2015. A three diode model for industrial solar cells and estimation of solar cell parameters using PSO algorithm. *Renew. Energy* 78, 105–113.

- Kler, D., Goswami, Y., Rana, K.P.S., Kumar, V., 2019. A novel approach to parameter estimation of photovoltaic systems using hybridized optimizer. *Energy Convers. Manage.* 187, 486–511.
- Kler, D., Sharma, P., Banerjee, A., Rana, K.P.S., Kumar, V., 2017. PV cell and module efficient parameters estimation using evaporation rate based water cycle algorithm. *Swarm Evol. Comput.* 35, 93–110.
- Kumar, C., Raj, T.D., Premkumar, M., Raj, T.D., 2020. A new stochastic slime mould optimization algorithm for the estimation of solar photovoltaic cell parameters. *Optik* 223, 165277.
- Liang, J.J., Qin, A.K., Suganthan, P.N., Baskar, S., 2006. Comprehensive learning particle swarm optimizer for global optimization of multimodal functions. *IEEE Trans. Evol. Comput.* 10 (3), 281–295.
- Lim, L.H.I., Ye, Z., Ye, J., Yang, D., Du, H., 2015. A linear identification of diode models from single I - V characteristics of PV panels. *IEEE Trans. Ind. Electron.* 62 (7), 4181–4193.
- Lin, X., Wu, Y., 2020. Parameters identification of photovoltaic models using niche-based particle swarm optimization in parallel computing architecture. *Energy* 196, 117054.
- Malekzadeh, M., Khosravi, A., Tavan, M., 2020b. A novel adaptive output feedback control for DC–DC boost converter using immersion and invariance observer. *Evol. Syst.* 11 (4), 707–715.
- Malekzadeh, M., Sadati, J., Alizadeh, M., 2016. Adaptive PID controller design for wing rock suppression using self-recurrent wavelet neural network identifier. *Evol. Syst.* 7 (4), 267–275.
- Mathew, D., Rani, C., Kumar, M.R., Wang, Y., Binns, R., Busawon, K., 2017. Wind-driven optimization technique for estimation of solar photovoltaic parameters. *IEEE J. Photovolt.* 8 (1), 248–256.
- Merchaoui, M., Sakly, A., Mimouni, M.F., 2018. Particle swarm optimisation with adaptive mutation strategy for photovoltaic solar cell/module parameter extraction. *Energy Convers. Manage.* 175, 151–163.
- Nasouri Gilvaei, M., Hosseini Imani, M., Jabbari Ghadi, M., Li, L., Golrang, A., 2021. Profit-based unit commitment for a GENC0 equipped with compressed air energy storage and concentrating solar power units. *Energy* 14 (3), 576.
- Nishioka, K., Sakitani, N., Uraoka, Y., Fuyuki, T., 2007. Analysis of multicrystalline silicon solar cells by modified 3-diode equivalent circuit model taking leakage current through periphery into consideration. *Sol. Energy Mater. Sol. Cells* 91 (13), 1222–1227.
- Niu, Q., Zhang, H., Li, K., 2014. An improved TLBO with elite strategy for parameters identification of PEM fuel cell and solar cell models. *Int. J. Hydrogen Energy* 39 (8), 3837–3854.
- Nunes, H.G.G., Pombo, J.A.N., Mariano, S.J.P.S., Calado, M.R.A., De Souza, J.F., 2018. A new high performance method for determining the parameters of PV cells and modules based on guaranteed convergence particle swarm optimization. *Appl. Energy* 211, 774–791.
- Oliva, D., Abd El Aziz, M., Hassani, A.E., 2017. Parameter estimation of photovoltaic cells using an improved chaotic whale optimization algorithm. *Appl. Energy* 200, 141–154.
- Oliva, D., Cuevas, E., Pajares, G., 2014. Parameter identification of solar cells using artificial bee colony optimization. *Energy* 72, 93–102.
- Ortiz-Conde, A., Sánchez, F.J.G., Muci, J., 2006. New method to extract the model parameters of solar cells from the explicit analytic solutions of their illuminated I - V characteristics. *Sol. Energy Mater. Sol. Cells* 90 (3), 352–361.
- Patel, S.J., Panchal, A.K., Kheraj, V., 2014. Extraction of solar cell parameters from a single current-voltage characteristic using teaching learning based optimization algorithm. *Appl. Energy* 119, 384–393.
- Pourmousa, N., Ebrahimi, S.M., Malekzadeh, M., Alizadeh, M., 2019. Parameter estimation of photovoltaic cells using improved lozi map based chaotic optimization algorithm. *Sol. Energy* 180, 180–191.
- Pourmousa, N., Ebrahimi, S.M., Malekzadeh, M., Gordillo, F., 2021. Using a novel optimization algorithm for parameter extraction of photovoltaic cells and modules. *Eur. Phys. J. Plus* 136 (4), 1–30.
- Qais, M.H., Hasani, H.M., Alghuwainem, S., 2019a. Identification of electrical parameters for three-diode photovoltaic model using analytical and sunflower optimization algorithm. *Appl. Energy* 250, 109–117.
- Qais, M.H., Hasani, H.M., Alghuwainem, S., 2020. Parameters extraction of three-diode photovoltaic model using computation and Harris Hawks optimization. *Energy* 195, 117040.
- Qais, M.H., Hasani, H.M., Alghuwainem, S., Nouh, A.S., 2019b. Coyote optimization algorithm for parameters extraction of three-diode photovoltaic models of photovoltaic modules. *Energy* 187, 116001.
- Rajasekar, N., Kumar, N.K., Venugopalan, R., 2013. Bacterial foraging algorithm based solar PV parameter estimation. *Sol. Energy* 97, 255–265.
- Rao, R., 2016. Jaya: A simple and new optimization algorithm for solving constrained and unconstrained optimization problems. *Int. J. Ind. Eng. Comput.* 7 (1), 19–34.
- Rizk-Allah, R.M., El-Fergany, A.A., 2020. Conscious neighborhood scheme-based Laplacian barnacles mating algorithm for parameters optimization of photovoltaic single-and double-diode models. *Energy Convers. Manage.* 226, 113522.
- Salahshour, E., Malekzadeh, M., Gholipour, R., Khorashadizadeh, S., 2019a. Designing multi-layer quantum neural network controller for chaos control of rod-type plasma torch system using improved particle swarm optimization. *Evol. Syst.* 10 (3), 317–331.
- Salahshour, E., Malekzadeh, M., Gordillo, F., Ghasemi, J., 2019b. Quantum neural network-based intelligent controller design for CSTR using modified particle swarm optimization algorithm. *Trans. Inst. Meas. Control* 41 (2), 392–404.
- Saleem, H., Karmalkar, S., 2009. An analytical method to extract the physical parameters of a solar cell from four points on the illuminated J - V curve. *IEEE Electron Device Lett.* 30 (4), 349–352.
- Selem, S.I., El-Fergany, A.A., Hasani, H.M., 2021. Artificial electric field algorithm to extract nine parameters of triple-diode photovoltaic model. *Int. J. Energy Res.* 45 (1), 590–604.
- Song, S., Wang, P., Heidari, A.A., Wang, M., Zhao, X., Chen, H., He, W., Xu, S., 2021. Dimension decided harris hawks optimization with Gaussian mutation: Balance analysis and diversity patterns. *Knowl.-Based Syst.* 215, 106425.
- Soon, J.J., Low, K.S., 2015. Optimizing photovoltaic model for different cell technologies using a generalized multidimension diode model. *IEEE Trans. Ind. Electron.* 62 (10), 6371–6380.
- Subudhi, B., Pradhan, R., 2017. Bacterial foraging optimization approach to parameter extraction of a photovoltaic module. *IEEE Trans. Sustain. Energy* 9 (1), 381–389.
- Toledo, F.J., Blanes, J.M., Galiano, V., 2018. Two-step linear least-squares method for photovoltaic single-diode model parameters extraction. *IEEE Trans. Ind. Electron.* 65 (8), 6301–6308.
- Tong, N.T., Pora, W., 2016. A parameter extraction technique exploiting intrinsic properties of solar cells. *Appl. Energy* 176, 104–115.
- Villalva, M.G., Gazoli, J.R., Ruppert Filho, E., 2009. Comprehensive approach to modeling and simulation of photovoltaic arrays. *IEEE Trans. Power Electron.* 24 (5), 1198–1208.
- Waly, H.M., Azazi, H.Z., Osheba, D.S., El-Sabbe, A.E., 2019. Parameters extraction of photovoltaic sources based on experimental data. *IET Renew. Power Gener.* 13 (9), 1466–1473.
- Wei, H., Cong, J., Lingyun, X., Deyun, S., 2011. Extracting solar cell model parameters based on chaos particle swarm algorithm. In: 2011 International Conference on Electric Information and Control Engineering. IEEE, pp. 398–402.
- Wolpert, D.H., Macready, W.G., 1997. No free lunch theorems for optimization. *IEEE Trans. Evol. Comput.* 1 (1), 67–82.
- Xu, S., Wang, Y., 2017. Parameter estimation of photovoltaic modules using a hybrid flower pollination algorithm. *Energy Convers. Manage.* 144, 53–68.
- Yahya-Khotbehsara, A., Shahhoseini, A., 2018. A fast modeling of the double-diode model for PV modules using combined analytical and numerical approach. *Sol. Energy* 162, 403–409.
- Ye, M., Wang, X., Xu, Y., 2009. Parameter extraction of solar cells using particle swarm optimization. *J. Appl. Phys.* 105 (9), 094502.
- Yousri, D., Thanikanti, S.B., Allam, D., Ramachandaramurthy, V.K., Eteiba, M.B., 2020. Fractional chaotic ensemble particle swarm optimizer for identifying the single, double, and three diode photovoltaic models' parameters. *Energy* 195, 116979.
- Yu, K., Liang, J.J., Qu, B.Y., Chen, X., Wang, H., 2017. Parameters identification of photovoltaic models using an improved JAYA optimization algorithm. *Energy Convers. Manage.* 150, 742–753.
- Yu, K., Qu, B., Yue, C., Ge, S., Chen, X., Liang, J., 2019. A performance-guided JAYA algorithm for parameters identification of photovoltaic cell and module. *Appl. Energy* 237, 241–257.
- Zekry, A., Shaker, A., Salem, M., 2018. Solar cells and arrays: Principles, analysis, and design. In: Advances in Renewable Energies and Power Technologies. Elsevier, pp. 3–56.